

A general theory of differentiated multicellularity

Felipe A. Veloso¹✉

¹Faculty of Biological Sciences, Universidad Andrés Bello, Santiago, Chile

✉Correspondence: veloso.felipe.a@gmail.com

Abstract

There is wide scientific consensus on the relevance of changes in the levels of gene expression for the cell differentiation process. Furthermore, research in the field has customarily assumed that such changes regulate this process when they interconnect in space and time by means of complex epigenetic mechanisms. Nevertheless, this assumed regulatory power lacks a clear definition and may even lead to logical inconsistencies. To tackle this problem, I analyzed publicly available high-throughput data of histone H3 post-translational modifications and mRNA abundance for different *Homo sapiens*, *Mus musculus*, and *Drosophila melanogaster* cell samples. Comprising genomic regions adjacent to transcription start sites, this analysis generated for each cell dataset a profile from pairwise partial correlations between histone modifications controlling for the respective mRNA levels. Here I report that these profiles, while explicitly uncorrelated to transcript abundance by construction, associate strongly with cell differentiation states. This association is not to be expected if cell differentiation is, in effect, regulated by epigenetic changes of gene expression. Based on these results, I postulate in this paper a falsifiable theory of differentiated multicellularity. This theory describes how the differentiated multicellular organism—understood as an intrinsic, higher-order, self-sufficient, self-repairing, self-replicating, and self-regulating dynamical constraint—emerges from proliferating undifferentiated cells. If it survives falsification tests consistently this theory would explain in principle (i) the self-regulated gene transcriptional changes during ontogeny and (ii) the emergence of differentiated multicellular lineages throughout evolution.

26 Introduction

27 The X-files of chromatin

28 Ontogeny, if seen as a motion picture in fast-forward, intuitively appears to be a teleological
29 process, its *telos*¹ being the multicellular organism in its mature form. The first step for a
30 scientific explanation of this apparent property was given in 1957 when Conrad Waddington
31 proposed his epigenetic landscape model. Influenced by earlier developments in dynamical
32 systems theory [1], Waddington’s model showed ontogeny to be potentially predictable or at least
33 potentially explainable without any teleological reference [2].

34 In practice however, system predictability has not been achieved yet, and research has rather
35 focused on “reverse engineering” the ontogenetic process from experimental results. Still, this
36 strategy has yielded remarkable results such as the induction of pluripotent stem cells (iPSCs) [3].
37 In terms of explainability, the dynamics of the cell differentiation process have been associated to
38 changes in chromatin states and concurrent heritable changes in gene expression levels, which
39 have been defined in turn as epigenetic changes [4, 5]). In some cases these changes can be
40 generated extrinsically with respect to the developing organism, as clearly observable in eusocial
41 insects (e.g. a female honeybee larva develops into a worker or a queen depending on the royal
42 jelly diet it is fed [6]). Nevertheless, most changes of gene expression during cell differentiation
43 are not only independent from, but are even robust with respect to extrinsic changes. This means
44 that ontogeny is fundamentally an intrinsically regulated process, for which no falsifiable theory
45 has emerged from the epigenetic framework since it was first advanced. Moreover, Peter Fraser
46 has recently referred to this problem as “The X-files of chromatin” [7].

47 This research work was conceived and designed to, following Fraser’s metaphor, declassify
48 “The X-files of chromatin”. In its initial phase, I conducted a computational analysis of the least
49 relevant—for the epigenetic landscape—constraints on histone H3 post-translational modification
50 states. Before outlining this analysis however, I must present here a case for the fundamental
51 impossibility of explaining the cell differentiation self-regulatory dynamics under the framework
52 pioneered by Waddington, however complex its underlying mechanisms may be (as also hinted
53 by Fraser [7]). Only then will I be able to argue that these epigenetically irrelevant constraints on
54 histone modification states are, in fact, key to a full understanding of differentiated multicellularity
55 in terms of its self-regulation and evolution.

56 The conundrum of self-regulation

57 Avoiding non-explanatory teleological descriptions, modern science regards cell differentiation
58 fundamentally as a dynamical system, where a fixed rule governs the transition between the
59 realizable states of a complex network of molecular mechanisms. Ranging from low-order
60 molecular interactions [8] to chromatin higher-order structural changes [9, 10], these mechanisms
61 propagate changes of gene expression in different loci as cells proliferate. Both heritable

¹τέλος is the Greek for “end”, “goal”, or “purpose”.

62 and uncorrelated to changes in the DNA sequence, these changes (defined as epigenetic as
63 mentioned previously) would in turn regulate cell differentiation. Furthermore, and although all
64 epigenetic mechanisms involved in cell differentiation are far from being completely elucidated,
65 the hypothesis that cell differentiation is regulated by epigenetic changes of gene expression
66 is routinely presented to the general public as a well-established scientific fact (as illustrated
67 in [11]). However, this hypothesis—whether or not we accept it in its strict sense—leads to severe
68 explanatory limitations and may even entail logical inconsistencies.

69 To assume the aforementioned hypothesis is true in its strict sense is to accept gene self-regulation
70 as a scientifically tenable and explainable teleological property of cell differentiation (the “intuitive”
71 *telos* here would be certain future transcriptional states to be timely achieved or maintained).
72 To explore what this implies let us suppose, for simplicity without loss of generality, that a
73 researcher modifies experimentally the expression levels of certain *geneA* and then elucidates how
74 those changes, during differentiation, activate or repress *geneB*, *geneC*, and *geneD*. At this point,
75 we might regard the finding as evidence that *geneB*, *geneC*, and *geneD* are regulated by *geneA*.
76 Consequently, we could also hold that *geneA* is a contributing part of the general regulatory
77 property. However, these assertions overlook that the researcher, not *geneA*, was the true regulator
78 by purposefully imposing certain transcriptional states (on *geneA*, and by means of *geneA*, also
79 *geneB*, *geneC*, and *geneD*). Yet, no human regulator is needed during the natural process, which
80 raises the question of what is the system truly regulating *geneA*, *geneB*, *geneC*, *geneD*, and by
81 extension, all genes during cell differentiation.

82 Moreover, explaining the regulation of transcriptional states in a gene locus by previous
83 transcriptional states in other gene loci (in the same cell or any other) is only an explanatory
84 regress. It takes the question about regulation, i.e. explaining a gene being at certain
85 transcriptional states (and, importantly, at no other transcriptional states), to some other gene
86 or genes, back in time. This regress inexorably leads—even in the simplest scenario—to the
87 unexplained, timely regulation of one key gene (or more key genes, simultaneously) within
88 undifferentiated cells.

89 On the other hand, to take the epigenetic-changes-regulate hypothesis in a loose sense is to
90 use “intrinsic regulation” only as a placeholder when referring to a certain class of molecular
91 mechanisms. If this is the case, we must note that any scientifically tenable mechanism requires
92 that the changes it comprises are at least dynamically correlated. In this context, an epigenetic
93 mechanism can be seen metaphorically as toppling dominoes (here the dynamically correlated
94 events are obvious). But as pointed out previously, this mechanism, however numerous or
95 intricately connected its correlated changes, says nothing about how the first domino tile (or
96 any other whose fall is not attributable to the fall of other tiles) was toppled over. To fill this
97 explanatory gap, it has been proposed that an “epigenator”—defined operationally as a transient
98 signal which probably originates in the environment of the cell—triggers the epigenetic phenotype
99 change after being transduced into the intracellular space [12]. Nonetheless, if all “epigenators” in
100 the system are extrinsic to it, by definition intrinsic regulation cannot be explained. On the other
101 hand, if there is at least one intrinsic “epigenator” in the system (e.g. a suggested “extracellular
102 signal”) its critical signaling property is left unexplained.

103 Importantly, these problems are inherent to *any* dynamical systems model intended to account
104 for the self-regulatory dynamics of cell differentiation. This is because any system able to explain
105 intrinsic “regulation” must be dynamically uncorrelated to the changes it “regulates”; otherwise
106 the “regulator” is, fundamentally, just another domino tile that propagates changes regardless
107 of its relative position. At this point the explanatory dead end becomes evident. Under the
108 traditional approach in developmental biology no higher-order system within a living organism,
109 however complex (e.g. displaying interlocked feedback loops or hypercyclic networks), exerts true
110 intrinsic regulation because its dynamics are ultimately correlated to the lower-order dynamics
111 it is supposed to regulate. Furthermore, in the epigenetic landscape any “intrinsic higher-order
112 regulator” can be no more than an epiphenomenon: a causally inefficacious system—whether or
113 not linear or predictable—resulting from molecular dynamics at the lowest level of scale.

114 **Epigenetic information in theory and practice**

115 Regardless of the explanatory limitations inherent to the traditional dynamical systems approach
116 in developmental biology, either all necessary information for cell differentiation is already
117 contained in the zygote or it is not. This dichotomy may seem to be trivial but important
118 implications follow it.

119 If the zygote contains all necessary information [13, 14], the previously discussed explanatory gap
120 could, in principle, be filled. Epigenetic imprinting, shown able to resolve a few early lineage
121 commitments in *Caenorhabditis elegans* [15], supports this possibility at first glance. Nevertheless,
122 a closer look at the complexity of this simple metazoan model suggests otherwise: *C. elegans*
123 ontogeny yields 19 different cell types (excluding the germ line) in a total of 1,090 generated cells.
124 From these two parameters alone, the required information capacity for the entire process can be
125 estimated to be at least 983 bit (see details in [Appendix](#)). Further, this is a great underestimation
126 since cell-fate uncertainty remains with respect two more variables at least, namely space and
127 time. In effect, cell-fate decisions are made in specific regions within the organism and/or
128 involve specific migration paths, and they are made in specific time points during differentiation.
129 Therefore, the non-genetic information capacity necessary for the entire process far exceeds the
130 few bits of information that epigenetic imprinting can account for.

131 Information not only requires a medium for its storage and transmission but also must have
132 content which, in this context, resolves the fate of every cell: apoptosis before division, division
133 without differentiation, or division with differentiation. Here an additional problem appears:
134 stem cell potency. An entire organism can develop (including extraembryonic tissues) from *any*
135 totipotent stem cell, and all embryonic tissues can develop from *any* pluripotent stem cell. How is
136 this possible if cell fate decisions are already specified deterministically in the zygote? The recently
137 proposed—yet not explanatory—“epigenetic disc” model for cell differentiation, under which the
138 pluripotent state is only one among many metastable and directly interconvertible states, reflects
139 the necessity to account for the context-dependent character of cell fate information [16].

140 With remarkable insight, in 1958 David L. Nanney anticipated explanatory pitfalls if the definition
141 of epigenetics is limited to heritable changes. He further stated that “‘cellular memory’ is
142 not an absolute attribute” [17]; or, in other words, that more important to development is

143 the process by which heritable material may manifest different phenotypes than the heritable
144 material itself. However, Waddington's epigenetic landscape prevailed and the field reinforced
145 a "preinformationist" framework: although the zygote is not a complete miniature version
146 of the mature organism (preformationism), it is indeed a complete blueprint of the mature
147 organism (allowing for some degree of extrinsic control, as in eusocial insects [6] and stochastic
148 gene expression [18]). If this is correct, we must also accept that in the mature human
149 brain—indisputably, one among many products of the developmental process—there is strictly
150 less non-genetic, non-redundant information than in the human zygote (not surprisingly however,
151 I failed to find a single research paper with such a proposition).

152 This *reductio ad absurdum* shows that the traditional dynamical systems approach (i.e. the
153 epigenetic landscape in developmental biology) has forced research to ignore or reject the
154 necessary *emergence* of not only some, but possibly most information content during ontogeny.
155 Specifically, if additional information content emerges during brain development, what would
156 necessarily preclude information content from emerging in proliferating undifferentiated
157 cells?

158 **A proof-of-principle hypothesis**

159 In the previous two subsections I argued that (i) explaining the self-regulatory dynamics of cell
160 differentiation under the traditional dynamical systems approach is a fundamental impossibility,
161 (ii) any intrinsic constraints regulating changes in gene expression during cell differentiation must
162 be dynamically uncorrelated to those changes, and (iii) any theory aiming to explain differentiated
163 multicellularity must account for emergent developmental information, which is not structurally
164 but dynamically embodied (that is, dependent on the extracellular context). Consequently, in this
165 work I designed a computational analysis to search for constraints as defined in (ii) because their
166 existence is, ultimately, the proof of principle for the theory referred to in (iii).

167 The specific objects of study were observed combinatorial constraints on histone H3
168 post-translational modifications (also known simply as histone H3 crosstalk). These modifications
169 were chosen because of their well-established statistical association with transcriptional states [19].
170 Notably, several high-throughput studies have underscored already the relevance of histone
171 crosstalk by identifying highly significant pairwise relationships between post-translational
172 modifications [20, 21, 22, 23].

173 Under these considerations, I defined the working hypothesis as follows: *for any cell population*
174 *in the same differentiation state and within genomic regions adjacent to transcription start sites,*
175 *constraints on histone H3 crosstalk explicitly uncorrelated to mRNA levels (i) are statistically*
176 *significant and (ii) associate with that differentiation state.* Importantly, the null hypothesis
177 (that is, no significant relationship exists between cell differentiation states and histone H3
178 crosstalk uncorrelated to mRNA levels) is further supported by the dynamical systems approach:
179 if heritable changes in mRNA levels explain completely cell differentiation states, an additional
180 non-epigenetic yet differentiation-associated level of constraints on histone H3 crosstalk is
181 superfluous.

182 For the computational analysis I used publicly available tandem datasets of ChIP-seq (chromatin
183 immunoprecipitation followed by high-throughput sequencing) on histone H3 modifications and
184 RNA-seq (transcriptome high-throughput sequencing) on mRNA for *Homo sapiens*, *Mus musculus*,
185 and *Drosophila melanogaster* (see [Materials and Methods](#)). Its basis was to define a numeric
186 profile *ctalk_non_epi*, which represents the strength and sign of pairwise partial correlations
187 between histone H3 modification states controlling for mRNA levels within genomic regions
188 adjacent to RefSeq transcription start sites. In other words, *ctalk_non_epi* profiles represent
189 the non-epigenetic component of pairwise histone H3 crosstalk in genomic regions where the
190 epigenetic component is significant.

191 The hypothesis testing rationale was to apply unsupervised hierarchical clustering on the
192 *ctalk_non_epi* profiles for different cell datasets in all three organisms, using non-parametric
193 bootstrap resampling to assess cluster significance [24]. If the null hypothesis is true, the obtained
194 clusters will be statistically insignificant, or else they will not associate with cell differentiation
195 states.

196 Results

197 In all analyses performed, *ctalk_non_epi* profiles fell into statistically significant clusters that
198 associate with cell differentiation states in *Homo sapiens*, *Mus musculus*, and *Drosophila melanogaster*.
199 Moreover, the results in detail suggest that *ctalk_non_epi* profiles associate with cell differentiation
200 states at least as strongly as do mRNA abundance² profiles (the relationship between
201 transcriptional and cell differentiation states is known and well-established [25, 26, 27]). In
202 summary, for all three organisms analyzed, the null hypothesis had to be consistently rejected,
203 indicating that the proof of principle described in the Introduction was obtained.

204 The embryonic stem cells *ctalk_non_epi* profile differs significantly from 205 those of differentiated cell types in *Homo sapiens*

206 Using data for nine different histone H3 modifications (for details see Materials and Methods),
207 *ctalk_non_epi* profiles were computed for six human cell types. From these, all profiles
208 corresponding to differentiated cell types, namely HSMM (skeletal muscle myoblasts), HUVEC
209 (umbilical vein endothelial cells), NHEK (epidermal keratinocytes), GM12878 (B-lymphoblastoids),
210 and NHLF (lung fibroblasts) fell into the largest statistically significant cluster. Such
211 significance was expressed in the obtained *au* (approximately unbiased) and *bp* (bootstrap
212 probability) significance scores, which were greater or equal than 95 (Figure 1A, cluster #4).
213 The *ctalk_non_epi* profile identified as dissimilar (i.e. excluded from the largest significant cluster)
214 was the one corresponding to H1-hESC embryonic stem cells.

215 For comparison and positive control, mRNA abundance profiles for the six cell types were
216 constructed from RNA-seq data (the same values that are controlled for in the computation
217 of *ctalk_non_epi* profiles) and then hierarchically clustered. As expected, the transcriptional
218 profile corresponding to H1-hESC (embryonic stem cells) was identified as significantly dissimilar,
219 i.e. resulted excluded from the largest significant cluster (Figure 1B, cluster #3), although in this
220 case it was excluded along with the GM12878 B-lymphoblastoids profile.

221 The *ctalk_non_epi* profiles associate with cell differentiation states in 222 *Mus musculus*

223 The analysis for mouse comprised five histone H3 modifications in five cell types. As in
224 *Homo sapiens* the *ctalk_non_epi* profiles fell into significant clusters that associate with
225 cell differentiation states. The five comprised cell type datasets were 8-weeks-adult heart,
226 8-weeks-adult liver, plus three datasets of E14 embryonic stem cells after zero, four, and six days
227 of differentiation respectively. All three E14 *ctalk_non_epi* profiles fell into a significant cluster
228 (Figure 1C, cluster #2) and within it, the profiles corresponding to latter time points (four and six
229 days of differentiation) fell into another significant cluster (Figure 1C, cluster #1). Additionally, the

²Represented by log₂-transformed FPKM values.

230 liver *ctalk_non_epi* profile was found to be more similar to the profiles of the least differentiated
231 states than the heart profile (Figure 1C, cluster #3).

232 Mouse mRNA abundance profiles also fell into significant clusters that associate with cell
233 differentiation states as expected (Figure 1D, clusters #1, #2 and #3). As *ctalk_non_epi* profiles
234 did, transcript abundance profiles resolved a significant difference between the earliest time point
235 (zero days of differentiation) and latter time points (Figure 1D, cluster #1).

236 **The *ctalk_non_epi* profiles associate with developmental periods and** 237 **time points in *Drosophila melanogaster***

238 In the final analysis, *ctalk_non_epi* profiles were computed from data for six histone H3
239 modifications in nine periods/time points throughout *Drosophila melanogaster* development
240 (0-4h, 4-8h, 8-12h, 12-16h, 16-20h and 20-24h embryos; L1 and L2 larval stages; pupae). As
241 observed in human and mouse profiles, fruit fly *ctalk_non_epi* profiles fell into clusters that
242 also associate strongly with the degree of cell differentiation (derivable from the degree of
243 development). One significant cluster grouped *ctalk_non_epi* profiles of earlier developmental
244 periods (Figure 1E, cluster #5) apart from later development profiles. Two more significant
245 clusters grouped later time point *ctalk_non_epi* profiles (Figure 1E, cluster #3) and separated the
246 L2 larvae profile (Figure 1E, cluster #7) from all other profiles.

247 General *ctalk_non_epi* cluster structure is not entirely consistent with developmental chronology
248 as the pupae profile (Figure 1E, cluster #7) shows. It must be noted however that, unlike
249 *Homo sapiens* and *Mus musculus* data where each *ctalk_non_epi* profile represented a specific or
250 almost specific differentiation state, each *Drosophila melanogaster* data set was obtained by the
251 authors from whole specimens (embryos, larvae and pupae). Especially for later development,
252 this implies that each *ctalk_non_epi* profile has to be computed from more than one partially
253 differentiated cell type at the same developmental period, thus limiting to a certain extent the
254 power of the analysis. This caveat in fact highlights the overall *ctalk_non_epi* cluster consistence
255 with developmental chronology, particularly when compared with that obtained from mRNA
256 levels as will be detailed next.

257 The mRNA abundance profiles in *D. melanogaster* yielded a general cluster structure much less
258 consistent with developmental chronology than the obtained from *ctalk_non_epi* profiles. For
259 example, the profile for 0-4h embryos fell into the same significant cluster with the profiles
260 for 16-20h and 20-24h embryos (Figure 1F, cluster #3). Additionally, the profile for 12-16h
261 embryos fell into the same significant cluster with the profiles for L1 and L2 larvae (Figure 1F,
262 cluster #5).

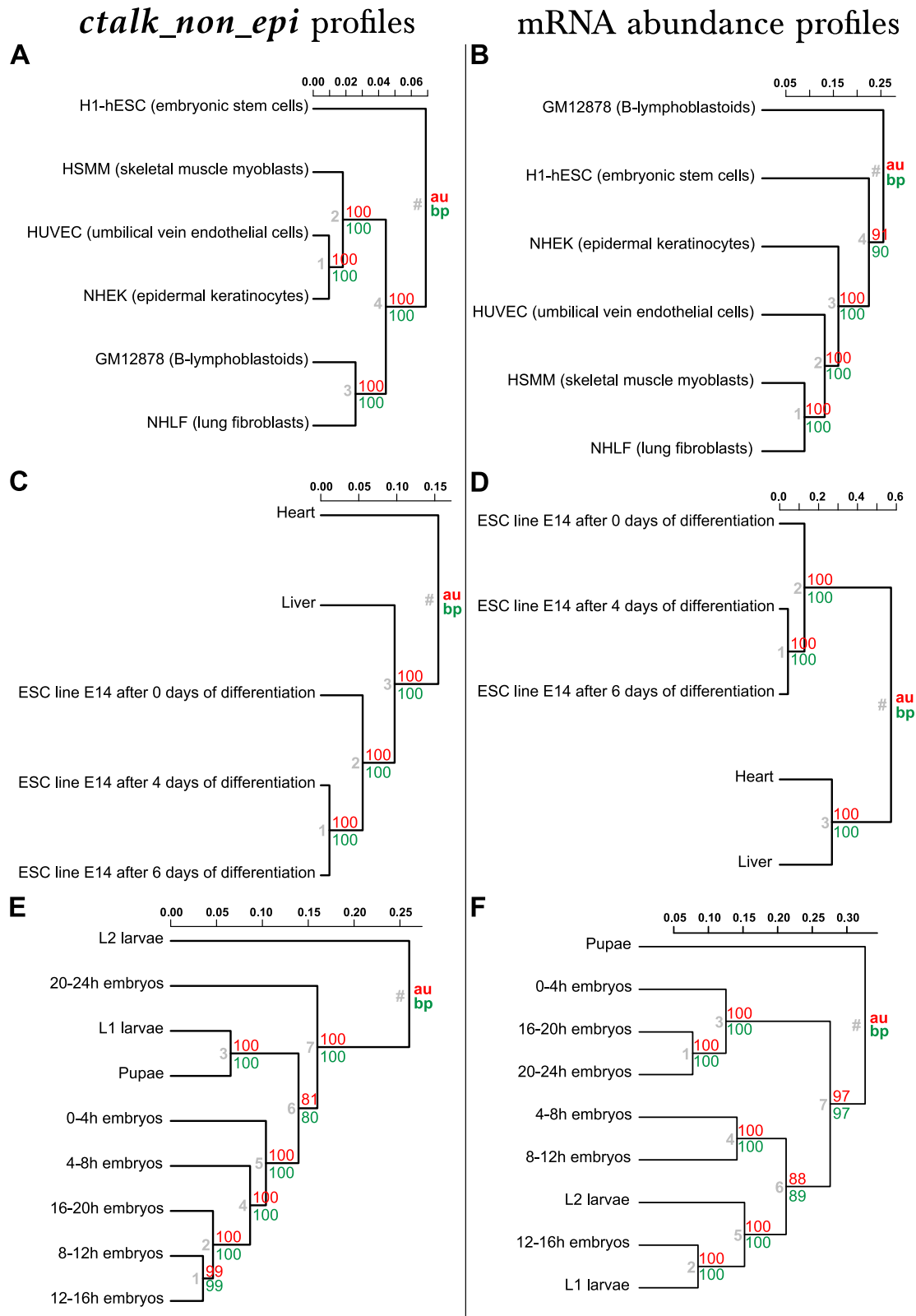


Figure 1: Unsupervised hierarchical clustering of *ctalk_non_epi* profiles and mRNA abundance profiles for *Homo sapiens* (A, B), *Mus musculus* (C, D), and *Drosophila melanogaster* (E, F). Metric: correlation (1 - r). Linkage method: “average” (also known as UPGMA). Significance scores [24]: **au** (approximately unbiased) and **bp** (bootstrap probability). Significant clusters were identified as those for which **au** and **bp** ≥ 95. Cluster numbers are in gray.

263 Discussion

264 Beyond the obtained proof of principle

265 The most important aspect of the previously presented results is not the clear and statistically
266 significant relationship between *ctalk_non_epi* profiles and cell differentiation states but instead
267 the nature of the constraints represented by *ctalk_non_epi* profiles (provided such relationship
268 exists). By definition, *ctalk_non_epi* profiles represent the strength and sign of pairwise partial
269 correlations computed from observed histone modification states; the same observed states that
270 previous research has shown able to predict transcriptional states with high accuracy ($R \sim 0.9$) [19].
271 It follows directly from these considerations that, for all three analyzed organisms within regions
272 adjacent to transcription start sites (henceforth TSSs), histone H3 modification states are subject
273 to an additional type of constraints that are explicitly uncorrelated to mRNA levels and associated
274 with cell differentiation states. In other words two systems, mutually uncorrelated and yet both
275 associated to cell differentiation, *simultaneously* constrain histone H3 modification states.

276 Still, any theory of differentiated multicellularity developed on the basis of the critique of the
277 traditional approach presented in the [introduction](#) and on the obtained proof of principle must
278 address these six fundamental questions:

279

280 **Q1** Since the constraints defining the proof of principle are explicitly uncorrelated to mRNA
281 levels by definition, how do they come to be associated with cell differentiation states?

282 **Q2** If they are indeed necessary for the intrinsic regulation of gene expression during cell
283 differentiation, how is such regulation exerted?

284 **Q3** Can these constraints be regarded as biologically meaningful information? If so, what is
285 the content of this information?

286 **Q4** Can they account for the remarkable and characteristic robustness of cell differentiation
287 with respect to even moderate perturbations?

288 **Q5** How do these constraints relate to the evolution of metazoans? Is this relationship
289 extendable to the evolution of other differentiated multicellular lineages such as plants?

290 **Q6** Are histone H3 modification states ultimately cause or effect of transcriptional states?
291 (This last question is a rehash of a very important point raised previously by Peter Fraser
292 and Wendy Bickmore [28].)

293 **Q7** Why undifferentiated cells start to differentiate in the embryo at certain time point?

294 **Problems with current views on the self-regulation of cell differentiation** 295 **and the evolution of multicellularity**

296 Since Ernst Haeckel’s “gastraea theory” [29], the explanatory accounts for the evolution of
297 multicellularity that are regarded as the most solid are fundamentally divorced from those aiming
298 to explain the dynamics of development such as the epigenetic landscape model. This is because
299 Haeckel’s hypothesis and the ones built upon it rely on the gradual specialization of same-species
300 (or even different-species [30]) cell colonies or aggregations [31, 32, 33, 34, 35], whereas ontogeny
301 and cell differentiation in particular start—in the development of every single multicellular
302 organism—from a single cell or, in other words, “from the inside out”. Although this divorce does
303 not necessarily preclude that the “colonial” approach points in the right direction, it is also clear
304 that a fundamental explanation for how a single cell came to embody this “dynamical reversal”
305 of development with respect to its evolutionary origin is lacking and will be needed.

306 Notably, some alternative “non-colonial” and “non-epigenetic” hypotheses have been advanced
307 aiming to explain the dynamics and informational requirements of cell-differentiation (which
308 in turn could provide some hints on the evolution of multicellularity). One of them is the
309 “darwinian cell differentiation” hypothesis by J. J. Kupiec, according to which gene expression
310 instability and stochasticity, in the context of external metabolic substrate gradients, creates
311 an intrinsic natural-selection-like mechanism able to drive the differentiation process [36].
312 Another “non-epigenetic” hypothesis, advanced by Andras Paldi, is that cell fate decisions are
313 the result of the characteristic coupling of gene expression and metabolism: fates are determined
314 by fluctuations in the nutrient/oxygen ratio, which are driven by the necessity to maintain
315 the dissipative nature of the metabolic network, which in turn must be redox-neutral at all
316 times [37].

317 At large, to my knowledge all explanatory accounts of the self-regulation of cell differentiation
318 and of the evolution of multicellularity suffer at least one of the following problems: (i) failure to
319 explain how structures or dynamics that supposedly account for the transition to multicellularity
320 or to cell differentiation have fundamentally analogous counterparts in unicellular lineages or
321 even prokaryotes, (ii) failure to account, at least in principle, for the information required
322 in cell fate decisions or in the transition between strictly single-cell-related content to
323 additional multicellular-individual-related content, (iii) failure to explain the reproducible and
324 robust self-regulatory dynamics—apart from the propagatory—of gene expression during cell
325 differentiation and, most importantly, (iv) unfalsifiability: this is why these accounts—importantly,
326 including the epigenetic landscape—are widely regarded as hypotheses, models, or frameworks
327 in spite of having been presented sometimes as theories by their authors.

328 In terms of overcoming these problems, it must be noted that Kupiec’s hypothesis encompassed a
329 variable that, I submit, is critical to the solution of the riddle: certain gradients in the extracellular
330 space—not yet identified, but both fundamentally conceivable and experimentally verifiable—can
331 be explicitly uncorrelated to gene expression profiles. It is possible that Kupiec did not consider
332 this possibility because his attempt to explain cell differentiation relied only on random variation
333 and selection, ruling out with this any explanatory role of emergent systems and properties.

334 In contrast to current hypotheses, the falsifiable theory to be postulated here regards the
335 multicellular organism as a higher-order system that *emerges* from proliferating undifferentiated
336 cells and *then* is subject to natural selection (as emerged the very first self-replicating and
337 self-repairing system—ancestor of all known living organisms—beyond any reasonable doubt).
338 Importantly, the theoretical development in this work is not based on the substrate-based³
339 concept of irreducible emergence (fundamentally refuted by Jaegwon Kim [38, 39]) but instead
340 converged (from the strict *explicitly-uncorrelated-dynamics* condition argued in the [introduction](#))
341 into what can be described as the constraint-based⁴ concept of emergence for higher-order
342 teleological systems, pioneered in a broader perspective by Terrence Deacon in 2011 [40].

³Understood as molecules and their realizable interactions, which define the state space in a dynamical systems model such as the epigenetic landscape.

⁴Understood as the dynamics explicitly *excluded* from realization in the system.

343 Preliminary theoretical definitions and notation

344 Before postulating the theory, I must introduce some new definitions and notation regarding
345 molecular dynamics and spatial topology. A brief glossary sufficient for the theoretical formulation
346 is provided below⁵.

347 **Context:** $X_{(i;t)}$ is the i^{th} cell of a given organism or cell population of the eukaryotic species
348 X at a given instant t . In the same logic, *the following concepts must be understood in*
349 *instantaneous terms and will be operationally treated as sets.*

350 S_E **Extracellular space:** The entire space in an organism or cell population that is
351 not occupied by the cells themselves at a given instant t . Positions in $S_E(t)$ will be
352 specified in spherical coordinates, namely r (radial distance), θ (azimuthal angle),
353 and ϕ (polar angle).

354 $C_W(X_{(i;t)})$ **Waddington's constraints:** The constraints associating certain subsets of the
355 spatially-specified molecular nuclear phenotype of $X_{(i;t)}$ with the instantaneous
356 transcription rates at the transcription start sites (TSSs), provided these
357 Waddington's constraints $C_W(X_{(i;t)})$ are *explicitly uncorrelated* with the genomic
358 sequence in dynamical terms.

359 $F_W(X_{(i;t)})$ **Waddington's embodyers:** The largest subset of the spatially-specified molecular
360 nuclear phenotype of $X_{(i;t)}$ for which the Waddington's constraints $C_W(X_{(i;t)})$ are
361 significant (e.g. histone H3 post-translational modifications in the TSS-adjacent
362 regions).

363 $F_W^{\rightarrow}(X_{(i;t)})$ **Waddington's extracellular propagators:** The largest subset of the entire
364 spatially-specified and membrane-exchangeable (by facilitated diffusion) molecular
365 phenotype of $X_{(i;t)}$ that excludes Waddington's embodyers $F_W(X_{(i;t)})$ but is capable
366 of eliciting a change—intracellular signal transduction may be required—in those
367 Waddington's embodyers $F_W(X_{(i;t)})$ after a certain time interval Δt .

368 $C_N(X_{(i;t)})$ **Nanney's constraints:** The constraints associating certain subsets of the
369 spatially-specified molecular nuclear phenotype of $X_{(i;t)}$ with the Waddington's
370 embodyers $F_W(X_{(i;t)})$, provided these Nanney's constraints $C_N(X_{(i;t)})$ are *explicitly*
371 *uncorrelated* with the instantaneous transcription rates at the TSSs in dynamical
372 terms.

373 $F_N(X_{(i;t)})$ **Nanney's embodyers:** The largest subset of the spatially-specified molecular
374 nuclear phenotype of $X_{(i;t)}$ for which the Nanney's constraints $C_N(X_{(i;t)})$ are
375 significant (e.g. histone H3 post-translational modifications in the TSS-adjacent
376 regions, as shown in the [Results](#)).

⁵The complete list of formal definitions and notation can be found in the [Appendix](#).

377 $F_N^{\rightarrow}(X_{(i;t)})$ **Nanney's extracellular propagators:** The subset of the entire spatially-specified
378 and membrane-exchangeable (by facilitated diffusion) molecular phenotype of
379 $X_{(i;t)}$ that excludes Nanney's embodiars $F_N(X_{(i;t)})$ but is capable of eliciting a
380 change—intracellular signal transduction may be required—in those Nanney's
381 embodiars $F_N(X_{(i;t)})$ after a certain time interval Δt .

382 **A general theory of differentiated multicellularity**

383 This theory mainly aims to explain how cell differentiation emerges in the ontogeny of extant
384 multicellular lineages and how differentiated multicellular lineages emerged throughout evolution.
385 To highlight the similarities of both phenomena at the most fundamental level, the theory will be
386 postulated in parts described in parallel. Each part will be described in terms of the evolution
387 of an ancestor eukaryotic species U towards differentiated multicellularity and in terms of
388 the ontogenetic process starting from the zygote of a differentiated multicellular species D .
389 Importantly, and although its proof of principle was obtained from high-throughput metazoan
390 data, this theoretical description makes no assumption whatsoever about a specific multicellular
391 lineage. This is why it is referred to as a general theory here and also in the title.

392
393 **Part I** **The unicellular and undifferentiated ancestor.** Let $U_{(i;t_{U_0})}$ be the i^{th} cell
394 **(Evolution)** in a population of the species U , which is the last unicellular eukaryotic
395 ancestor species of the extant differentiated multicellular species D . Here
396 the spatially-specified phenotype $F(U_{(i;t_{U_0})})$ displays Waddington's embodyers
397 (i.e. $F_W(U_{(i;t_{U_0})}) \neq \emptyset$, e.g. histone post-translational modifications) but cell
398 differentiation is not possible. Also, significant constraints exist between the
399 entire spatially-specified phenotype $F(U_{(i;t_{U_0})})$ and Waddington's propagators
400 $F_W(U_{(i;t_{U_0})})$ regardless of $T(U_{(i;t_{U_0})})$ (i.e. significant Nanney's constraints
401 $C_N(U_{(i;t_{U_0})})$ exist). However, Nanney's propagators (if any) are confined to
402 $U_{(i;t_{U_0})}$. In other words, here Nanney's extracellular propagators do not exist
403 (i.e. $F_N^{\rightarrow}(U_{(i;t_{U_0})}) = \emptyset$; see **Figure 2A**, top)

404 **Part I** **The multicellular organism's zygote.** Let $D_{(1;t_{D_0})}$ be a zygote of the extant
405 **(Ontogeny)** differentiated multicellular species D . Like $F(U_{(i;t_{D_0})})$, the spatially-specified
406 phenotype $F(D_{(1;t_{D_0})})$ displays Waddington's embodyers (i.e. $F_W(D_{(1;t_{D_0})}) \neq \emptyset$,
407 e.g. histone post-translational modifications) but cell differentiation is
408 not observed *yet*. Also, significant constraints exist between the entire
409 spatially-specified phenotype $F(D_{(1;t_{D_0})})$ and Waddington's propagators
410 $F_W(D_{(1;t_{D_0})})$ regardless of $T(D_{(1;t_{D_0})})$ (i.e. significant Nanney's constraints
411 $C_N(D_{(1;t_{D_0})})$ exist). But unlike in $U_{(i;t_{D_0})}$, Nanney's propagators are *not* confined
412 to $D_{(1;t_{D_0})}$. In other words, here Nanney's extracellular propagators do exist
413 (i.e. $F_N^{\rightarrow}(D_{(1;t_{D_0})}) \neq \emptyset$; see **Figure 2A**, bottom).

414
415 **Part II** **The necessary novel alleles.** At some instant $(t_M - \Delta t_M) > t_{U_0}$ during
416 **(Evolution)** evolution the genome $G(U_{(k;t_M - \Delta t_M)})$ of certain k^{th} cell of the species U changes
417 such that at least one element of its associated phenotype is specifiable in the set
418 of Nanney's extracellular propagators (i.e. $F_N^{\rightarrow}(U_{(k;t_M - \Delta t_M)}) \neq \emptyset$). As remarked
419 in the previous subsection, this implies that $G(U_{(k;t_M - \Delta t_M)})$ accounts also for
420 all other phenotypic gene products necessary for the facilitated diffusion of the
421 molecule(s) specified in $F_N^{\rightarrow}(U_{(k;t_M - \Delta t_M)})$. Importantly, the novel alleles involved

422 in the change $G(U_{(i;t_{U_0})}) \rightarrow G(U_{(k;t_M-\Delta t_M)})$ (**Figure 2A to 2B**) are a necessary
 423 but not sufficient condition for differentiated multicellularity (**Figure 2B**).

424 **Part II**
 425 **(Ontogeny)**

426 **The already present necessary alleles.** At any instant $(t_D - \Delta t_D) > t_{D_0}$
 427 preceding cell differentiation, the genome specified by $G(D_{(i;t_D-\Delta t_D)})$ (i.e. any
 428 daughter cell in the embryo) is similar to $G(U_{(k;t_M-\Delta t_M)})$ (see **Figure 2B**) in
 429 the sense that both genomes code for Nanney’s extracellular propagators
 430 (i.e. the sets $F_N^{\rightarrow}(D_{(i;t_D-\Delta t_D)})$ and $F_N^{\rightarrow}(U_{(k;t_M-\Delta t_M)})$ are nonempty). Importantly,
 431 the alleles specified in the zygote’s genome $G(D_{(1;t_{D_0})})$ and in $G(D_{(i;t_D-\Delta t_D)})$
 432 (i.e. the genome of any of its daughter cells) are a necessary but not sufficient
 433 condition for cell differentiation.

433 **Part III**
 434 **(Evolution &**
 435 **Ontogeny)**

436 **Diffusion flux of Nanney’s extracellular propagators and the geometry**
 437 **of the extracellular space S_E .** The existence of Nanney’s extracellular
 438 propagators F_N^{\rightarrow} in any cell population $\{X_{(1;t)}, \dots, X_{(n;t)}\}$ (i.e. cells
 439 of the species X at any given instant t) implies that a scalar field⁶
 440 $\Phi_N(X_{(1;t)}, \dots, X_{(n;t)}, r, \theta, \phi) \geq 0$ can represent the concentration of Nanney’s
 441 extracellular propagators in $S_E(X_{(1;t)}, \dots, X_{(n;t)})$. When the number of cells is
 442 small enough, diffusion flux is fast enough to overtake the spatial constraints
 443 imposed by the relatively simple geometry of $S_E(X_{(1;t)}, \dots, X_{(n;t)})$. Under
 444 these conditions the associated gradient⁷ $\vec{\nabla} \Phi_N(X_{(1;t)}, \dots, X_{(n;t)}, r, \theta, \phi) =$
 445 $\left(\frac{\partial \Phi_N(X_{(1;t)}, \dots, X_{(n;t)}, r, \theta, \phi)}{\partial r}, \frac{1}{r} \frac{\partial \Phi_N(X_{(1;t)}, \dots, X_{(n;t)}, r, \theta, \phi)}{\partial \theta}, \frac{1}{r \sin \theta} \frac{\partial \Phi_N(X_{(1;t)}, \dots, X_{(n;t)}, r, \theta, \phi)}{\partial \phi} \right)$
 446 remains in magnitude⁸ under a certain critical value V_M in $S_E(X_{(1;t)}, \dots, X_{(n;t)})$
 447 for the daughter cells of $U_{(k;t_M-\Delta t_M)}$ and under a critical value V_D for the
 448 differentiated multicellular species D . Importantly, the constraints represented
 449 in the gradient $\vec{\nabla} \Phi_N(X_{(1;t)}, \dots, X_{(n;t)}, r, \theta, \phi)$ imply there is free energy
 450 available—whether or not there is cell differentiation—which, as will be
 451 described later, is in fact partially utilized as work in the generation of new
 452 information content.

⁶A scalar field is a function associating a scalar (here concentration of Nanney’s extracellular propagators F_N^{\rightarrow}) to every point in space.

⁷The gradient vector field $\vec{\nabla}$ of a scalar function (in this context, the scalar field Φ_N) is a vector operation that generalizes the concept of derivative represented by the differential operator—denoted by the ∇ (nabla) symbol and also called “del”—to more than one dimension.

⁸Note that in spherical coordinates the magnitude of the gradient is simply the partial derivative of the scalar field $\Phi_N(X_{(1;t)}, \dots, X_{(n;t)}, r, \theta, \phi)$ (concentration of Nanney’s extracellular propagators F_N^{\rightarrow}) with respect to the radial distance: $|\vec{\nabla} \Phi_N(X_{(1;t)}, \dots, X_{(n;t)}, r, \theta, \phi)| = \frac{\partial \Phi_N(X_{(1;t)}, \dots, X_{(n;t)}, r, \theta, \phi)}{\partial r}$.

450 **Part IV**
451 **(Evolution)**

452 **The emergent transition to differentiated multicellularity.** At some later
453 but relatively close instant t_M , cell proliferation yields a significantly
454 larger population. Now diffusion flux of Nanney's extracellular propagators
455 is no longer able to overtake the increasing spatial constraints in
456 the extracellular space S_E . A significant gradient, in magnitude equal
457 or greater—anywhere in S_E —than the critical value V_M forms then,
458 i.e. $\left| \vec{\nabla} \Phi_N(\mathbf{U}_{(1;t_M)}, \dots, \mathbf{U}_{(n;t_M)}, r, \theta, \phi) \right| \geq V_M, (r, \theta, \phi) \in S_E$. Therefore, Nanney's
459 extracellular propagators F_N^{\rightarrow} diffuse differentially into each cell, yielding
460 unprecedented differential Nanney's constraints $\{C_N(\mathbf{U}_{(1;t_M)}), \dots, C_N(\mathbf{U}_{(n;t_M)})\}$
461 in the cells' nuclei by virtue of no cell or gene product in particular
462 but, importantly, of the constraints imposed by the entire proliferating cell
463 population on the diffusion flux of F_N^{\rightarrow} in S_E . These differential Nanney's
464 constraints are in turn defined with respect to Waddington's embodyers
465 $\{F_W(\mathbf{U}_{(1;t_M)}), \dots, F_W(\mathbf{U}_{(n;t_M)})\}$, thus they now constrain the instantaneous
466 transcription rates $\{T(\mathbf{U}_{(1;t_M)}), \dots, T(\mathbf{U}_{(n;t_M)})\}$ in a differential and dynamically
uncorrelated manner (**Figure 2C**). This is how multicellular lineages, displaying
self-regulated changes of gene expression during ontogeny, evolved.

467 **Part IV**
468 **(Ontogeny)**

469 **The emergent transition to cell differentiation.** At some later but
470 relatively close instant t_D , embryonic growth yields certain number
471 of undifferentiated cells. Now diffusion flux of Nanney's extracellular
472 propagators is no longer able to overtake the increasing spatial constraints
473 in the extracellular space S_E . A significant gradient, in magnitude equal
474 or greater—anywhere in S_E —than the critical value V_D forms then,
475 i.e. $\left| \vec{\nabla} \Phi_N(\mathbf{D}_{(1;t_D)}, \dots, \mathbf{D}_{(n;t_D)}, r, \theta, \phi) \right| \geq V_D, (r, \theta, \phi) \in S_E$ (see question Q7).
476 Therefore, Nanney's extracellular propagators F_N^{\rightarrow} diffuse differentially
477 into each cell, yielding unprecedented differential Nanney's constraints
478 $\{C_N(\mathbf{D}_{(1;t_D)}), \dots, C_N(\mathbf{D}_{(n;t_D)})\}$ in the cells' nuclei by virtue of no cell
479 or gene product but, importantly, of the constraints imposed by the
480 entire growing embryo on the diffusion flux of Nanney's extracellular
481 propagators in the extracellular space S_E . These differential Nanney's
482 constraints are in turn defined with respect to Waddington's embodyers
483 $\{F_W(\mathbf{D}_{(1;t_D)}), \dots, F_W(\mathbf{D}_{(n;t_D)})\}$, thus they now constrain the instantaneous
484 transcription rates $\{T(\mathbf{D}_{(1;t_D)}), \dots, T(\mathbf{D}_{(n;t_D)})\}$ in a differential and dynamically
485 uncorrelated manner (**Figure 2C**). This is how undifferentiated cells start
486 to differentiate, displaying self-regulated changes of gene expression during
ontogeny (see question Q1).

487 **Part V**
488 **(Evolution)**

489 **What was the evolutionary breakthrough?** Since the oldest undisputed
490 differentiated multicellular organisms appear in the fossil record around
491 2.8 billion years after the first stromatolites [41], the necessary microevolutionary
492 represented by $G(\mathbf{U}_{(i;t_{U_0})}) \rightarrow G(\mathbf{U}_{(k;t_M - \Delta t_M)})$ can be safely regarded as a
highly improbable step. Nevertheless, the major evolutionary breakthrough
was not genetic but instead the unprecedented dynamical regime emerging

493 from proliferating eukaryote cells at t_M , or in more general terms at
494 $\{t_{M_1}, \dots, t_{M_n}\}$ throughout evolution since extant differentiated multicellular
495 organisms constitute a paraphyletic group [42, 33]. This novel dynamical regime
496 emerges as a higher-order constraint⁹ from the synergistic coupling of the
497 lower-order Waddington's constraints C_W and Nanney's constraints C_N (able
498 now to propagate through the extracellular space S_E). Although dependent on
499 the alleles in $G(U_{(k;t_M-\Delta t_M)})$ to emerge given enough cell proliferation, this
500 system is not a network of epigenetic mechanisms—however complex—but
501 instead a particular instantiation of a *teleodynamic system*, proposed by Terrence
502 Deacon in his *theory of emergence by constraint coupling and preservation*¹⁰ [40],
503 which is presented to and shaped by natural selection at each instant. In this
504 context, environmental constraints as oxygen availability [43] and even gravity
505 (see [Corollary #5](#)) filter out specific emergent multicellular dynamics that are
506 incompatible with them. In summary, the critical evolutionary novelty was
507 the unprecedented multicellular *self*, which can be described as an intrinsic,
508 higher-order, self-sustaining, self-repairing, self-replicating, and self-regulating
509 dynamical constraint on individual eukaryotic cells.

510 Part V 511 (Ontogeny)

Who is regulating cell differentiation? Contrary to what could be
512 expected under the “top-down causation” framework (common to earlier
513 formulations of causally efficacious emergent properties, and fundamentally
514 refuted [38, 39] as mentioned previously), the theory hereby postulated does
515 *not* regard the proliferation-generated extracellular gradient $\vec{\nabla}\Phi_N$ such that
516 $|\vec{\nabla}\Phi_N(D_{(1;t_D)}, \dots, D_{(n;t_D)}, r, \theta, \phi)| \geq V_D, (r, \theta, \phi) \in S_E$ as the fundamental
517 regulator of the cell differentiation process. While differential Nanney's
518 constraints $\{C_N(D_{(1;t_D)}), \dots, C_N(D_{(n;t_D)})\}$ are *regulatory constraints* with respect
519 to Waddington's embodyers $\{F_W(D_{(1;t_D)}), \dots, F_W(D_{(n;t_D)})\}$ (as described in
520 [Part IV-Ontogeny](#)), the reciprocal proposition is also true: since Waddington's
521 constraints $\{C_W(D_{(1;t_D)}), \dots, C_W(D_{(n;t_D)})\}$ are dynamically uncorrelated to
522 Nanney's extracellular propagators $\{F_N^{\rightarrow}(D_{(1;t_D)}), \dots, F_N^{\rightarrow}(D_{(n;t_D)})\}$ (e.g. changes
523 in the expression of the protein pores or carriers necessary for the facilitated
524 diffusion of Nanney's extracellular propagators). *If and only if the dynamically*
525 *uncorrelated Waddington's constraints C_W and Nanney's constraints C_N ¹¹ become*
526 *synergistically coupled across the extracellular space S_E true intrinsic regulation on*
527 *the cell differentiation process is possible.* This implies in turn that both chromatin
528 states and transcriptional states are simultaneously cause and effect with respect
529 to each other (this regime, intuitively describable as “chicken-egg” dynamics, is
530 the answer this theory provides to question Q6). Ontogenic self-regulation is
531 then exerted by the intrinsic higher-order constraint or *teleodynamic system* that

⁹Understood as the states explicitly excluded from being realized in the dynamics of the system.

¹⁰Although Deacon himself named his theory *emergent dynamics*, I am proposing here this longer but more descriptive name.

¹¹Both emerge in turn from genetic (i.e. structurally embodied) constraints.

532 emerges from proliferating cells. In other words, the differentiated multicellular
533 organism *is* the causally efficacious, higher-order, coupled constraint emerging
534 from and regulating *ipso facto* Nanney's constraints C_N and Waddington's
535 constraints C_W in what would be otherwise a population or colony—however
536 symbiotic—of individual eukaryotic cells (see question Q2).
537

538 **Part VI**
539 **(Evolution)**

Unprecedented multicellular dynamics. Once the necessary
539 microevolutionary change $G(U_{(i;t_{D_0})}) \rightarrow G(U_{(k;t_M-\Delta t_M)})$ took place in
540 the species U phenomena like gene duplication or alternative splicing¹² made
541 possible the appearance of a plethora of novel multicellular (*teleodynamic*)
542 regimes and consequently novel cell types, tissues and organs. Moreover, the
543 dependence of differentiated multicellularity on one or more coexisting $\vec{\nabla}\Phi_N$
544 gradients (i.e. constraints on diffusion flux) in S_E , which importantly depend
545 on no cell in particular but on the entire cell population or embryo, yields
546 at least two important implications in evolutionary terms. First, it explains
547 in principle the remarkable robustness of differentiated multicellularity with
548 respect to extrinsic perturbations (see question Q4). Second, since a higher-order
549 constraint is taking over the regulation of changes in gene expression within
550 individual cells, it is predictable that said cells lose some cell-intrinsic systems
551 that were critical in a time when eukaryotic life was only unicellular, even when
552 compared with their prokaryotic counterparts¹³. In this context a result obtained
553 over a decade ago acquires relevance. In a genome-wide study comprising ~ 90
554 bacterial and ~ 10 eukaryote species, it was found that the number of genes
555 involved in transcriptional change increases as a power law of the total number
556 of genes [44], with an exponent of 1.87 ± 0.13 for bacteria. Remarkably, the
557 corresponding exponent for eukaryotes was closer to one (i.e. to linearity):
558 1.26 ± 0.10 . The previously described loss of lower-order, cell-intrinsic regulatory
559 systems in differentiated multicellular organisms—by virtue of emergent $\vec{\nabla}\Phi_N$
560 gradients in S_E —is entirely consistent with this observation.

561 **Part VI**
562 **(Ontogeny)**

What does ontogeny recapitulate? This theory holds the hereby proposed
562 emergent transition, spontaneous from cell proliferation shortly after Nanney's
563 extracellular propagators $F_N^{\vec{\nabla}}$ appeared, as key to the evolution of any
564 multicellular lineage displaying self-regulated changes of gene expression
565 during cell differentiation. Therefore, it rejects in turn the hypothesis that
566 metazoans—or, in general, any multicellular lineage displaying self-regulated
567 cell differentiation—evolved from gradual specialization of single-cell colonies
568 or aggregations [29, 31, 32, 33, 34, 35]. Importantly however, this is not to
569 argue that potentially precedent traits (e.g. cell-cell adhesion) were necessarily
570 unimportant for the later fitness of differentiated multicellular organisms.
571 Neither is this to reject Haeckel's famous assertion completely: in every extant

¹²In the loci involved in the synthesis and/or facilitated diffusion of Nanney's extracellular propagators $F_N^{\vec{\nabla}}$.

¹³T. Deacon generically described this as the offloading of teleodynamic constraints in lower-order systems—at the cost of losing teleodynamic properties—into the higher-order teleodynamic system emerging from them.

572 multicellular lineage this self-sufficient, self-repairing, self-replicating, and
573 self-regulating system has emerged over and over again from undifferentiated
574 cells and presented itself to natural selection ever since its evolutionary debut.
575 Therefore, at least in this single yet most fundamental sense, ontogeny does
576 recapitulate phylogeny.
577

578 **Part VII**
579 **(Evolution &**
580 **Ontogeny)**

The role of epigenetic changes. Contrary to what the epigenetic landscape model entails, under this theory the heritable changes of gene expression do not define let alone explain the intrinsic regulation of cell differentiation. The robustness, heritability, and number of cell divisions which any epigenetic change comprises are instead adaptations of the higher-order dynamical constraint emergent from individual cells (i.e. the multicellular organism). These adaptations have been shaped by natural selection after the emergence of each extant multicellular lineage and are in turn reproduced or replaced by novel adaptations in every successful ontogenetic process.

588 **Part VIII**
589 **(Evolution &**
590 **Ontogeny)**

Novel cell types, tissues and organs evolve and develop. Further microevolutionary changes in the alleles specified in $G(U_{(k;t_M-\Delta t_M)})$ or already present in $G(D_{(1;t_{D_0})})$ (e.g. gene duplication, alternative splicing) imply than one or more than one $\{\vec{\nabla}\Phi_{N_1}, \dots, \vec{\nabla}\Phi_{N_k}\}$ gradients emerge in S_E with cell proliferation. A cell type T_j will develop then in a region S_{E_i} of the extracellular space S_E when a relative uniformity of Nanney's extracellular propagators is reached, i.e. $\left(\left|\vec{\nabla}\Phi_{N_1;T_j}\right|, \dots, \left|\vec{\nabla}\Phi_{N_k;T_j}\right|\right) \leq \left(V_{N_1;T_j}, \dots, V_{N_k;T_j}\right), (r, \theta, \phi) \in S_{E_i}$ (see a two-cell-type and two-gradient depiction in **Figure 2D**). As highlighted earlier, cell differentiation is not *regulated* by these gradients themselves but by the higher-order constraint emergent from their synergistic coupling with Waddington's constraints C_W within the cells. This constraint synergy can be exemplified as follows: gradients $\{\vec{\nabla}\Phi_{N_1}, \dots, \vec{\nabla}\Phi_{N_k}\}$ can elicit changes of gene expression in a number of cells, which in turn may promote the dissipation of the gradients (e.g. by generating a surrounding membrane that reduces dramatically the effective S_E size) or may limit further propagation of those gradients from S_E into the cells (e.g. by repressing the expression of protein pores or carriers involved in the facilitated diffusion of $F_N^{\vec{\nabla}}$ in S_E). Thus, under this theory cell types, tissues, and organs evolved sequentially as “blobs” of relatively small magnitude $F_N^{\vec{\nabla}}$ gradients in regions $\{S_{E_i}, \dots, S_{E_n}\}$ within S_E (as just described) displaying no particular shape. These “blobs” emerged with no function in particular—apart from not being incompatible with the multicellular organism's survival and reproduction—by virtue of random genetic variation (involved in the embodiment and propagation of Nanney's constraints C_N) followed by cell proliferation. Then, the “blobs” were shaped by natural selection from their initially random physiological and structural properties to specialized cell types, tissues, and organs (importantly, such specialization evolves with respect to the

614 emergent intrinsic higher-order constraint postulated here as the multicellular
615 organism). The result of this evolutionary process is observable in the dynamics
616 that emerge during the ontogeny of extant multicellular species (**Figure 2E**).

617
618 **Part IX**
619 **(Evolution &**
620 **Ontogeny)**

621 **Emergent information content and multicellular self-repair.** As argued in
622 the introduction, a significant amount of information content has to *emerge* to
623 account for robust and reproducible cell fate decisions and for the self-regulated
624 dynamics of cell differentiation in general. Under this theory, this content
625 emerges when the significant gradient or gradients $\{\vec{\nabla}\Phi_{N_1}, \dots, \vec{\nabla}\Phi_{N_k}\}$ form at
626 some point from proliferating undifferentiated cells, entangling synergistically
627 Nanney’s constraints C_N and Waddington’s constraints C_W across S_E . Crucially,
628 this information is *not* about any coding sequence and its relationship with
629 cell-intrinsic and cell-environment dynamics (i.e. genetic information) *nor* about
630 any heritable gene expression level/profile and its relationship with cell-intrinsic
631 and cell-environment dynamics (i.e. epigenetic information). Instead, this
632 information is *about the multicellular organism as a whole* (understood as the
633 emergent higher-order intrinsic constraint described previously) and also about
634 the environmental constraints under which this multicellular organism develops.
635 For this reason I propose to call this emergent information *hologenic*¹⁴ (see
636 question Q3). No less importantly, at each instant the multicellular organism is
637 not only interpreting hologenic information—by constraining its development
638 into specific trajectories since it emerges—but also actively creating novel
639 hologenic information (in other words displaying “chicken-egg” dynamics,
640 similar to those described in **Part V-Ontogeny**). In the multicellular organism,
641 the subset of the molecular phenotype that conveys hologenic information is
642 not only the subset involved in the gradients $\{\vec{\nabla}\Phi_{N_1}, \dots, \vec{\nabla}\Phi_{N_k}\}$ but the entire
643 subset embodying or propagating Nanney’s constraints C_N . Additionally, since
644 the gradients $\{\vec{\nabla}\Phi_{N_1}, \dots, \vec{\nabla}\Phi_{N_k}\}$ depend on no cell in particular—not even on
645 a sufficiently small group of cells—but on the whole cell population or embryo,
cell differentiation will be robust with respect to moderate perturbations such as
some cell loss (see question Q4).

646 **Part X**
647 **(Ontogeny)**

648 **Ontogeny ends and cell differentiation “terminates”.** If under this theory
649 cell differentiation emerges with the proliferation of (at the beginning,
650 undifferentiated) cells, why should it terminate for any differentiation lineage?
651 What is this “termination” in fundamental terms? These are no trivial questions.
652 As an answer to the first, zero net proliferation begs the fundamental
653 question. To the second, a “fully differentiated” cell state condition fails
654 to explain the existence of adult stem cells. To address these issues three
considerations are most important: (i) for any cell or group of cells the molecules
specifiable as Nanney’s extracellular propagators F_N^{\rightarrow} at any instant t may

¹⁴ὅλος is the ancient Greek for “whole” or “entire”.

not be specifiable as such at some later instant¹⁵ $t + \Delta t$, (ii) the emergent *telos* or “end” in this theory is the instantaneous, higher-order intrinsic constraint that emerges from proliferating undifferentiated cells (i.e. the multicellular *self*); *not* a *telos* such as the organism’s mature form, a fully differentiated cell, or certain future transcriptional changes to achieve such states (described as “intuitive” in the [introduction](#)), which are logically inconsistent¹⁶ and unjustifiably homuncular and, (iii) this causally-efficacious, higher-order constraint emerges from the synergistic coupling of lower-order Waddington’s constraints C_W and Nanney’s constraints C_N across the extracellular space S_E . Therefore, under this theory, cell differentiation “terminates” (the quotes will be justified below) in any given region S_{E_i} of the extracellular space if a stable or metastable equilibrium is reached where (i) the gradients of Nanney’s extracellular propagators dissipate in S_{E_i} under certain critical values, i.e. $\left(\left| \vec{\nabla} \Phi_{N_1} \right|, \dots, \left| \vec{\nabla} \Phi_{N_k} \right| \right) < (V_{D_1}, \dots, V_{D_k}), (r, \theta, \phi) \in S_{E_i}$ ([Figure 2F](#), left) and/or (ii) those gradients are unable to constrain Waddington’s embodiments F_W in the cells’ nuclei because the critical gene products (protein pores/carriers or intracellular transducers) are non-functional or not expressed, i.e. when the cells become “blind” to the gradients ([Figure 2F](#), right). Condition (i) can be reached for example when development significantly changes the morphology—increasing the surface-to-volume ratio—of the cells. This is because such increase removes spatial constraints in S_E that facilitate the emergence/maintenance of the gradients. It is thus predictable under this theory a significant positive correlation between the degree of differentiation of a cell and its surface-to-volume ratio, once controlling for characteristic length (i.e. “unidimensional size”) and also a negative significant correlation between stem cell potency/regenerative capacity and that ratio. On the other hand, condition (ii) can be reached when the cell differentiation process represses at some point the expression of the protein pores or carriers necessary for the facilitated diffusion of the *current* Nanney’s extracellular propagators F_N^{\rightarrow} . Importantly, the stability of the equilibrium required in these conditions will depend on the cells’ currently expressed phenotype, e.g. an adult multipotent or pluripotent stem cell—in stark contrast to a fully differentiated neuron—may differentiate if needed [45] and some differentiated cell may dedifferentiate given certain stimuli [46]. These examples underscore that the *telos* of cell differentiation is not a “fully differentiated” state but, as this theory explains, the instantaneous, intrinsic higher-constraint which is the multicellular organism as a whole. Consequently, the “termination” of cell differentiation should be understood rather as an indefinite-as-long-as-functional stop, or even as apoptosis. The multicellular *telos* described will prevail in ontogeny (and did prevail in evolution) as long as an even higher-order *telos* does not emerge from it (e.g. once a central nervous system develops/evolved).

¹⁵This exemplifies why the [theoretical definitions and notation](#) had to be developed in instantaneous terms.

¹⁶Since such a *telos* entails the causal power of future events on events preceding them.

695 **Part X**
696 **(Evolution)**

697 The evolutionarily-shaped *telos*. Whereas the causal power of the organism's
698 mature form as ontogenetic *telos* is logically untenable and only apparent, the
699 assumption that the zygote is a complete developmental blueprint containing
700 all necessary information for the process—as argued in the [introduction](#)—is
701 also untenable. In contrast, ontogeny is, under this theory, an emergent,
702 evolutionarily-shaped and truly (instantaneously) teleological process. The reason
703 why it intuitively appears to be “directed” to and by the organism's mature
704 form is that the intrinsic higher-order constraint—the true (instantaneous) *telos*
705 described previously—and the hologenic information content emerging along
706 with it are exerting, instant after instant, causal power on the ontogenetic process.
707 Although the propagation of constraints within this process (e.g. propagated
708 changes of gene expression) is decomposable into molecular interactions, its
709 teleological causal power (e.g. self-regulation) is not. This is because its *telos*
710 is a spontaneous, intrinsic higher-order *constraint* or “thermodynamic zero”
711 emergent from lower-order constraints; it cannot be reduced or decomposed
712 into molecular interactions—as the arithmetic zero cannot be divided and for
713 the same fundamental reason—as T. Deacon first argued [40]. This is also why
714 hologenic content (and in general any information content, as Deacon has argued
715 as well) is thermodynamically *absent* or constrained: hologenic content is not
716 in the molecular substrates conveying that content anymore than the content
717 of this theory is in integrated circuits, computer displays, paper, or even in the
718 complex neural interactions within the reader's brain. As described previously in
719 less specific terms, what becomes constrained (i.e. thermodynamically “*absent*”)
720 in the dynamics of the multicellular organism is the content of hologenic
721 information (see question [Q3](#)); the substrates propagating the critical constraints
722 for this change can only then be identified as conveying hologenic information.
723 Natural selection has thus shaped the content of hologenic information by
724 shaping the genetic constraints it is ultimately emergent from, not any particular
725 molecules or molecular interactions as media, which should be regarded in this
726 context as means to the *telos*, as the etymology indirectly implies. Moreover,
727 the necessary microevolutionary change $G(U_{(i;t_0)}) \rightarrow G(U_{(k;t_M-\Delta t_M)})$ (described
728 in [Part II-Evolution](#)) could well have been significantly smaller—in terms of
729 gene or protein sequence similarity—than the total changes undergone between
730 $G(U_{(i;t_0)})$ and some of its own eukaryotic unicellular ancestors. In general,
731 accounting for substantial differences in the phenotype and its properties¹⁷ given
732 comparatively small genetic changes is bound to be an intractable task if one or
733 more teleodynamic transitions during evolution is/are involved yet ignored.

732 In hindsight, the [description](#) for the evolution of cell types, tissues and organs
733 based on initial “blobs” of relative F_N^{\rightarrow} uniformity in S_E together with the
734 predicted positive correlation between degree of cell differentiation and cell
735 surface-to-volume ratio suggest an additional and more specific evolutionary
736 implication. That is, the high surface-to-volume ratio morphology needed

¹⁷When great, these differences usually involve intrinsically teleological dynamics at a variety of levels, e.g. function, regulation, courtship, or planning.

737 for neuron function—and possibly neuron function itself—was only to be
738 expected in the evolution of multicellularity and is only to be expected in
739 multicellular-like life (if any) elsewhere in the Universe, provided no rigid
740 wall (of high relative fitness) impedes the tinkering with substantial increases
741 of the cells surface-to-volume ratio, as observable in plants. In turn this
742 caveat—now together with the predicted negative correlation between stem cell
743 potency and surface-to-volume ratio—suggests that if a multicellular lineage
744 is constrained to always display low cell surface-to-volume ratios, stem cell
745 potency and regenerative capacity will be higher. All other things being equal,
746 these multicellular lineages should be characterized then by a comparatively
747 lower complexity but also by longer lifespan and more robustness to extrinsic
748 damage (see question [Q5](#)).
749
750

751 The synergy in the coupling of Waddington’s constraints C_W and Nanney’s constraints C_N
752 across S_E described in this theory does not preclude that cell differentiation may display phases
753 dominated by proliferation and others dominated by differentiation itself: whereas significant
754 gradients of Nanney’s extracellular propagators F_N^{\rightarrow} in S_E emerge at some point given enough
755 cell proliferation, it is also true that the exchange of such propagators between the cells and S_E
756 is constrained by the dynamics of facilitated diffusion which, importantly, are saturable. Any
757 representative computer simulation of cell differentiation according to this theory, however
758 simple, will depend on an accurate modeling of the lower-order dynamical constraints it emerges
759 from.

760 Importantly, this theory also encompasses coenocytic (also commonly called “syncytial”) stages of
761 development, where cell nuclei divide in absence of cytokinesis (observable in some invertebrates
762 such as *Drosophila*). In such stages, Nanney’s extracellular propagators have to be operationally
763 redefined as Nanney’s *extranuclear* propagators, while still maintaining their fundamental defining
764 property.

765 In terms of results indirectly related to this theory, it must be noted that evidence has already been
766 found for tissue migration across a self-generated chemokine gradient in zebrafish [47, 48]. This
767 finding demonstrates the feasibility of some of the dynamics proposed here, namely eukaryotic
768 cells utilizing certain free energy (available in the spontaneous constraints on diffusion in S_E
769 generated by cell migration/proliferation) as work in their own intrinsic dynamics. These two
770 linked processes—one spontaneous, the other non-spontaneous—exemplify a work cycle as
771 proposed by Stuart Kauffman [49]. What remains to be verified is the synergistic coupling of two
772 (as in this theory) or more constraint systems, as proposed by T. Deacon, into the higher-order
773 constraint or multicellular organism described here.

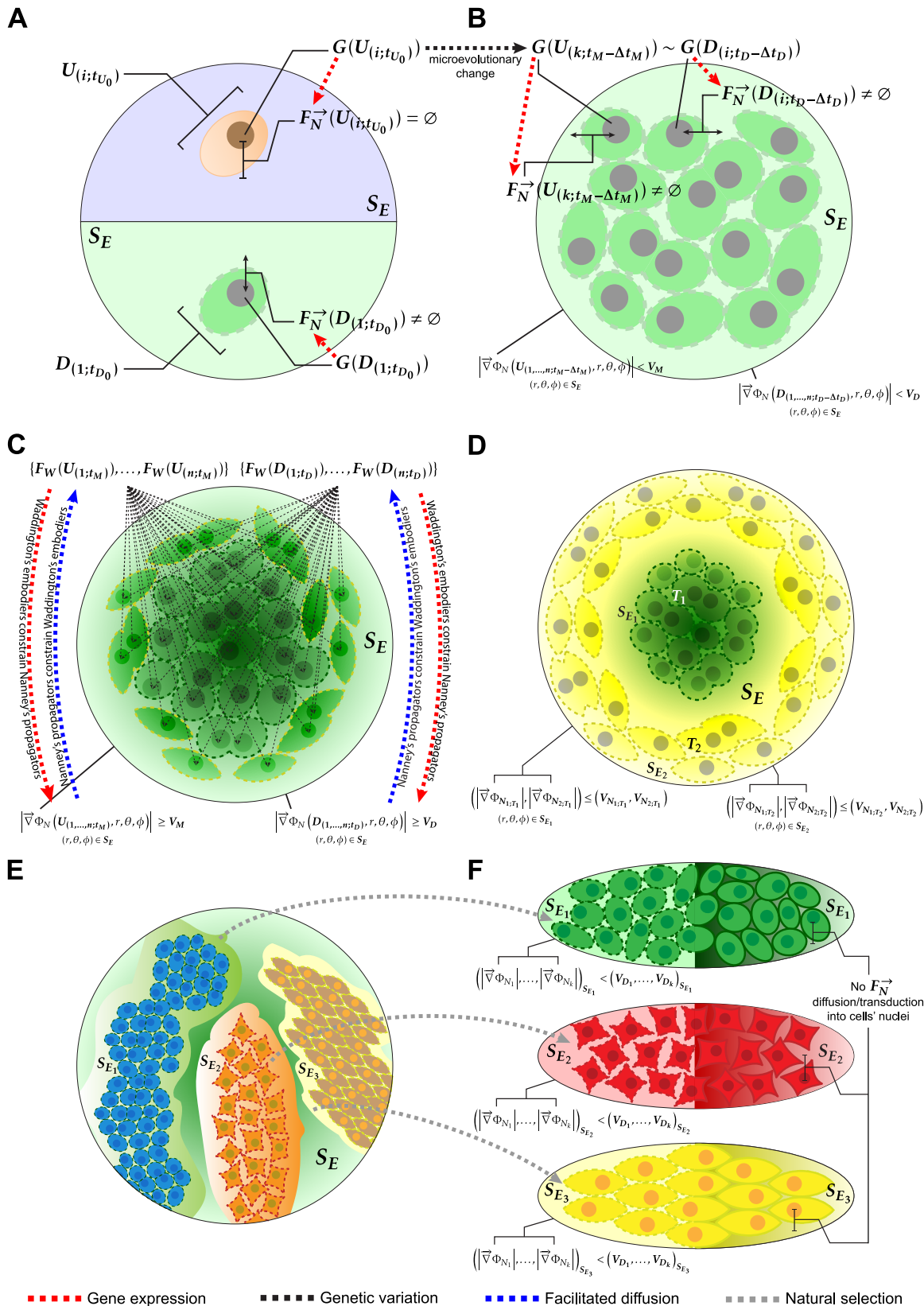


Figure 2: Main steps in the theory: 1. The unicellular and undifferentiated ancestor (A, top) and the zygote (A, bottom). 2. The necessary alleles are present and cells proliferate, but still no significant $\nabla\Phi_N$ gradients form in S_E (B). 3. The multicellular *telos* (i.e. intrinsic higher-order constraint) emerges when significant $\nabla\Phi_N$ gradients couple the lower-order C_N and C_W constraints synergistically across S_E (C). 4. Two cell types start to develop in differential regions with relative $\nabla\Phi_N$ uniformity (D). 5. Cell types/tissues/organs evolve as emergent “blobs” of relatively small $\nabla\Phi_N$ magnitude and then are shaped by natural selection (E). 6. Cell differentiation stops when $\nabla\Phi_N$ gradients dissipate (F, left) or when they cannot diffuse/be transduced into the cells’ nuclei (F, right).

774 Falsifiability

775 Popper's criterion of falsifiability will be met in this paper by providing the two following
776 experimentally-testable predictions:

- 777 1. Under the proposed theory, the gradient $\vec{\nabla} \Phi_N(\mathbf{D}_{(1;t)}, \dots, \mathbf{D}_{(n;t)}, r, \theta, \phi)$ such that
778 $\left| \vec{\nabla} \Phi_N(\mathbf{D}_{(1;t_D)}, \dots, \mathbf{D}_{(n;t_D)}, r, \theta, \phi) \right| \geq V_D, (r, \theta, \phi) \in S_E$ is a necessary condition for the
779 emergence of cell differentiation during ontogeny. It follows directly from this proposition
780 that *if undifferentiated or differentiating cells are extracted continuously from a developing*
781 *embryo at the same rate they are proliferating*, then at some instant $t_D + \Delta t$ the
782 gradient of Nanney's extracellular propagators in S_E will dissipate by virtue of the
783 Second Law of thermodynamics, reaching everywhere values under the critical value,
784 i.e. $\left| \vec{\nabla} \Phi_N(\mathbf{D}_{(1;t_D+\Delta t)}, \dots, \mathbf{D}_{(n;t_D+\Delta t)}, r, \theta, \phi) \right| < V_D, (r, \theta, \phi) \in S_E$. Thus, as long as cells
785 are extracted, *the undifferentiated cells will not differentiate or the once differentiating cells*
786 *will enter an artificially-induced diapause or developmental arrest*. A proper experimental
787 control will be needed for the effect of the cell extraction technique itself (that is, applying
788 it to the embryo but extracting no cells).
- 789 2. *There is a significant positive correlation between the cell-wise or cell-type-wise dissimilarity of*
790 *Nanney's embodyers F_N in an embryo and developmental time, which will be observable given*
791 *enough resolution in the experimental technique*. In practical terms, totipotent stem cells can
792 be taken from an early-stage embryo and divided into subsamples, and embryos from
793 later stages in the same species can be divided (e.g. by cryosection [50]) into subsamples.
794 Then, ChIP-seq on histone H3 modifications and RNA-seq on mRNA can be used to obtain
795 the corresponding *ctalk_non_epi* profile—which represent Nanney's constraints C_N on
796 histone H3 modifications (adjacent to TSSs) as embodyers—for each subsample. If the
797 predicted correlation fails to be observed even using single-cell high-throughput sequencing
798 methods [51], the theory postulated here should be regarded as falsified.
- 799 3. *If any molecular substrate M (i) is specifiable as a Nanney's extracellular propagator*
800 *during a certain time interval for certain cells of a differentiated multicellular species*
801 *(see Corollary #1) and (ii) is also synthesized by an unicellular eukaryote species U that is*
802 *unable to differentiate* (e.g. the dinoflagellate *Lingulodinium polyedrum* [52]), then *experiments*
803 *will fail to specify M as a Nanney's extracellular propagator for the species U .*

804 Corollaries

805 Described next are some corollaries, hypotheses and predictions (not involving falsifiability) that
806 can be derived from the theory.

807 **1. Nanney’s extracellular propagators.** The strongest prediction that follows from the
808 theory is the existence of Nanney’s extracellular propagators, i.e. $F_N^{\vec{}} \neq \emptyset$ for any
809 differentiated multicellular species D . Since these propagators are instantaneously defined,
810 their identification should be in the form “molecule M is specifiable as a Nanney’s
811 extracellular propagator of the species D in the cell, cell population, or cell type T_i at
812 the developmental time point t (or the differentiation state s)”. This will be verified if,
813 for example, an experiment shows that the *ctalk_non_epi* profiles in these T_i cell or cells
814 vary significantly when exposed to differential concentrations of M in the extracellular
815 medium. If this is the case, it is also predictable that M will be synthesized by the cells *in*
816 *vivo* at a relatively constant rate (at least as long as M is specifiable as $F_N^{\vec{}}$ for them).
817 Importantly, there is no principle in this theory precluding a molecular substrate M from
818 being specifiable as $F_N^{\vec{}}$ and also as Waddington’s extracellular propagator $F_W^{\vec{}}$ ¹⁸. Note:
819 although the existence of Nanney’s extracellular propagators is a very strong and verifiable
820 prediction, it was not included in the [previous subsection](#) because it is not falsifiable in a
821 strict epistemological sense.

822 **2. Surface-to-volume ratio and the evolution and development of the extracellular**
823 **matrix.** It was proposed earlier ([Part X-Evolution](#)) an important relationship between
824 cell surface-to-volume ratio and the evolution of differentiated multicellularity, in
825 particular between the neuron’s high surface-to-volume ratio and the evolution of its
826 function. Importantly, under the predicted relationship between regenerative capacity
827 and surface-to-volume ratio (see [Part X-Ontogeny](#)) neuron-shaped cells are expected to
828 be the most difficult to regenerate. This would have been the (developmental) price to
829 pay for a higher-order, dynamically faster form of multicellular *self* (i.e. higher-order
830 intrinsic constraint) that neurons—whose interconnectivity is underpinned by their high
831 surface-to-volume ratio—make possible. On the other hand glial cells (companions of
832 neurons in the nervous tissue) have a smaller surface-to-volume ratio than neurons so
833 they would support them by constraining to some extent the diffusion flux of Nanney’s
834 extracellular propagators $F_N^{\vec{}}$ in the neurons “effective” extracellular space¹⁹. Notably, the
835 glial cells with the smallest surface-to-volume ratio are ependymal cells, which have been
836 found able to serve as neural stem cells [53]. Since this analysis is based on constraints and
837 not on specific material embodiments, the logic of the neurons and glial cells example can
838 be extended to the evolution and development of the extracellular matrix in general. That
839 is, the extracellular matrix was not only shaped by natural selection making it provide the
840 cells structural and biochemical support but also developmental support, understood as
841 fine-tuned differential constraints to the diffusion flux of Nanney’s extracellular propagators

¹⁸This dual specifiability is not unlikely, since the synergistic coupling of Waddington’s constraints C_W and Nanney’s constraints C_N across S_E requires that at least one type of molecular substrates is simultaneously specifiable as Waddington’s embodiens F_W and Nanney’s embodiens F_N .

¹⁹Understood in this case as the neuroglia plus the neural extracellular matrix.

842 F_N^{\rightarrow} in S_E . Moreover, I submit that the evolution of this developmental support probably
843 preceded the evolution of all other types of support, given the critical role of the F_N^{\rightarrow}
844 gradients in the emergence and preservation of the multicellular *telos*.

845 **3. Natural developmental arrests or diapauses.** The account for natural
846 diapauses—observable in arthropods [54] and some species of killifish
847 (Cyprinodontiformes) [55]—in this theory follows directly from the description
848 in [Part X-Ontogeny](#). That is, natural diapauses are a metastable equilibrium state
849 characterized by (i) the dissipation of Nanney’s extracellular propagators F_N^{\rightarrow} in S_E
850 under certain critical values (e.g. if some factor inhibits cell proliferation) or (ii) the
851 inability of these gradients to constrain Waddington’s embodyers F_W in the cells’ nuclei
852 because the critical gene products (protein pores/carriers or intracellular transducers) are
853 non-functional or not expressed. For example, if in some organism the function of the
854 protein pores/carriers critical for the facilitated diffusion of the current F_N^{\rightarrow} is temperature
855 dependent, then at that time development will enter a diapause given certain thermal
856 conditions and resume when those conditions are lost.

857 **4. F_N^{\rightarrow} gradients and tissue regeneration.** Whereas the scope of the theory
858 is the dynamics of cell differentiation and the evolution of differentiated
859 multicellularity, it may provide some hints about other developmental processes
860 such as tissue regeneration after extrinsic damage. For instance, I hypothesize
861 that an important constraint driving the regenerative response to wounds (e.g.
862 a cut in the skin) is the gradient $\left| \vec{\nabla} \Phi_N(D_{(1;t_{\text{wound}})}, \dots, D_{(n;t_{\text{wound}})}, r, \theta, \phi) \right| \gg$
863 $\left| \vec{\nabla} \Phi_N(D_{(1;t_{\text{wound}}-\Delta t)}, \dots, D_{(n;t_{\text{wound}}-\Delta t)}, r, \theta, \phi) \right|$, $(r, \theta, \phi) \in S_E$ generated by the wound
864 itself. This is because a cut creates an immediate, significant gradient at the wound
865 edges (evidence has been already found for extracellular H_2O_2 gradients mediating
866 wound detection in zebrafish [56]). If relevant variables (such as F_N^{\rightarrow} diffusivity in the
867 extracellular space S_E , see [Corollary #2](#)) prevent this gradient from dissipating quickly, it
868 should contribute to a developmental regenerative response as it dissipates gradually. If
869 different tissues of the same multicellular individual are compared, a significant negative
870 correlation should be observable between the regenerative capacity after injury in a tissue
871 and the average cell surface-to-volume ratio in that tissue, once controlling for average cell
872 characteristic length.

873 **5. Effects of microgravity on development.** In the last few decades a number of abnormal
874 effects of microgravity on development-related phenomena—including mammal tissue
875 culture [57], plant growth [58], human gene expression [59], cytoskeleton organization and
876 general embryo development ([60] and references therein)—have been described. A general
877 explanation proposed for these effects is that microgravity introduces a significant degree of
878 mechanical perturbation on critical structures for cells and tissues which as a whole would
879 be the “gravity sensors” [61]. Without dismissing these structural perturbations as relevant,
880 I suggest that a key perturbation on development elicitable by microgravity is a significant
881 alteration—with respect to standard gravity—of the instantaneous F_N^{\rightarrow} distribution in
882 the extracellular space S_E . This could be explained in turn by changes in the diffusion
883 dynamics (as evidence for changes in the diffusion of miscible fluids suggest [62]) and/or a

884 significant density difference between the extracellular space S_E and the cells.

885 6. **Why plant seeds need water.** It is a well-known fact that plant seeds only need certain
886 initial water intake to be released from dormancy and begin to germinate with no further
887 extrinsic support. Whereas this specific requirement of water has been associated to embryo
888 expansion and metabolic activation of the seeds [63, 64], I submit that it is also associated
889 to the fundamental need for a medium in S_E where the critical $F_N \vec{\nabla}$ gradients can emerge.
890 This is because such gradients are in turn required for the intrinsic regulation of the
891 asymmetric divisions already shown critical for cell differentiation in plants [65].

892 **Concluding remarks**

893 The analysis conducted to search for the theoretical proof of principle in this work encompassed
894 two relevant simplifications or approximations: gene expression levels were represented
895 theoretically by instantaneous transcription rates, which in turn were approximated by mRNA
896 abundance in the analysis. These steps were justified since (i) the correlation between gene
897 expression and mRNA abundance has been clearly established as positive and significant
898 in spite of the limitations of the techniques available [66, 67], (ii) if gene expression can be
899 accurately expressed as a linear transformation of mRNA abundance as the control variable, the
900 *ctalk_non_epi* profiles will remain unchanged (see details in [Materials and Methods](#)) and, (iii) the
901 association between *ctalk_non_epi* profiles and cell differentiation states was robust with respect
902 to these simplifications and approximations as shown in the [Results](#).

903 If the theory advanced here is ever tested and resists falsification attempts consistently,
904 further research will be needed to identify the cell-and-instant-specific Nanney's extracellular
905 propagators F_N^{\rightarrow} at least for each multicellular model organism, and also to identify the
906 implications (if any) of this theory on other developmental processes such as aging or diseases
907 such as cancer. Also, more theoretical development will be needed to quantify the capacity and
908 classify the content of hologenic information that emerges along with cell differentiation.

909 On the other hand, I wish to underscore that the critique of the epigenetic landscape approach
910 presented in the [introduction](#) (in terms of its supposed ability to explain the self-regulatory
911 dynamics of cell differentiation) is completely independent from a potential falsification of
912 the theory. Even that being the case, I argue that if future research keeps on elucidating the
913 mechanisms propagating changes of gene expression to an arbitrarily high level of detail—while
914 failing to recognize that the constraints that truly regulate changes²⁰ must be dynamically
915 uncorrelated yet coupled to the constraints that propagate those changes—advances in the
916 fundamental understanding of the evolution and self-regulatory dynamics of differentiated
917 multicellularity will not be significant.

918 What underpins this view is that scientifically tenable (i.e. instantaneous) teleological dynamics
919 in nature—unless we are still willing to talk about intrinsically teleological concepts like
920 function, regulation, agency, courtship or planning in all fields of biology while holding
921 they are fundamentally meaningless—must be dynamically uncorrelated to the lower-order
922 dynamics they emerge from. Furthermore, the only way such requisite can be fulfilled is that an
923 intrinsic higher-order constraint emerges from the synergistic coupling of lower-order constraints,
924 as Terrence Deacon first proposed. Whereas these thermodynamically spontaneous, intrinsic
925 constraints are dependent on molecular substrates embodying, propagating, and coupling them
926 at any instant, these substrates can be added, replaced or even dispensed with at any instant
927 as long as the *telos* is preserved. For all these reasons, the differentiated multicellular organism
928 described in this theory (and any living system in general) is no mechanism or machine of
929 any type (e.g. autopoietic [68])—interconnecting in this case a eukaryotic cell population—for
930 mechanisms and machines fundamentally entail an *explicit correlation* between the dynamics
931 within them.

²⁰Whatever those constraints are if not the ones described in this theory.

932 Thus, the emergence of differentiated multicellularity throughout evolution and in every successful
933 ontogenetic process has been—and still is—the emergence of unprecedented, constraint-based,
934 thermodynamic *selves* in the natural world; *selves* which no machine or mechanism could
935 ever be.

936 **Materials and Methods**

937 **Data collection**

938 The genomic coordinates of all annotated RefSeq TSSs for the hg19 (*Homo sapiens*), mm9
939 (*Mus musculus*), and dm3 (*Drosophila melanogaster*) assemblies were downloaded from the UCSC
940 database. Publicly available tandem datafiles of ChIP-seq²¹ on histone H3 modifications and
941 RNA-seq²² for each analyzed cell sample in each species were downloaded from the ENCODE,
942 modENCODE or NCBI's SRA databases [69, 70, 71, 72, 73, 74, 75].

943 The criteria for selecting cell type/cell sample datasets in each species was (i) excluding those
944 with abnormal karyotypes or lacking available RNA-seq data and (ii) among the remaining
945 datasets, choosing the group that maximizes the number of specific histone H3 modifications
946 shared. Under these criteria, the comprised cell type/sample datasets in this work were thus:

947
948 ***H. sapiens*** 6 cell types: HSMM (skeletal muscle myoblasts), HUVEC (umbilical
949 vein endothelial cells), NHEK (epidermal keratinocytes), GM12878
950 (B-lymphoblastoids), NHLF (lung fibroblasts) and H1-hESC (embryonic stem
951 cells).

952 9 histone H3 modifications: H3K4me1, H3K4me2, H3K4me3, H3K9ac,
953 H3K9me3, H3K27ac, H3K27me3, H3K36me3, and H3K79me2.

954 ***M. musculus*** 5 cell types: 8-weeks-adult heart, 8-weeks-adult liver, E14-day0 (embryonic
955 stem cells after zero days of differentiation), E14-day4 (embryonic stem cells
956 after four days of differentiation), and E14-day6 (embryonic stem cells after
957 six days of differentiation).

958 5 histone H3 modifications: H3K4me1, H3K4me3, H3K27ac, H3K27me3, and
959 H3K36me3.

960 ***D. melanogaster*** 9 cell samples: 0-4h embryos, 4-8h embryos, 8-12h embryos, 12-16h embryos,
961 16-20h embryos, 20-24h embryos, L1 larvae, L2 larvae, and pupae.

962 6 histone H3 modifications: H3K4me1, H3K4me3, H3K9ac, H3K9me3,
963 H3K27ac, and H3K27me3.

964
965 See [Supplementary Information](#) for the datafile lists in detail.

²¹Comprising 1x36bp, 1x50bp, and 1x75bp reads, depending on the data series (details available via GEO accession codes listed in [Supplementary Information](#)).

²²Comprising 1x36bp, 1x100bp, and 2x75bp reads, depending on the data series (details available via GEO accession codes listed in [Supplementary Information](#)).

966 **ChIP-seq read profiles and normalization**

967 The first steps in the EFilter algorithm by Kumar *et al.*—which predicts mRNA levels in
968 log-FPKM (fragments per transcript kilobase per million fragments mapped) with high accuracy
969 ($R \sim 0.9$) [19]—were used to generate ChIP-seq read signal profiles for the histone H3 modifications
970 data. Namely, (i) dividing the genomic region from 2kbp upstream to 4kbp downstream of each
971 TSS into 30 200bp-long bins, in each of which ChIP-seq reads were later counted; (ii) dividing the
972 read count signal for each bin by its corresponding control (Input/IgG) read density to minimize
973 artifactual peaks; (iii) estimating this control read density within a 1-kbp window centered on
974 each bin, if the 1-kbp window contained at least 20 reads. Otherwise, a 5-kbp window, or else
975 a 10-kbp window was used if the control reads were less than 20. When the 10-kbp length was
976 insufficient, a pseudo-count value of 20 reads per 10kbp was set as the control read density.
977 This implies that the denominator (i.e. control read density) is at least 0.4 reads per bin. When
978 replicates were available, the measure of central tendency used was the median of the replicate
979 read count values.

980 **ChIP-seq read count processing**

981 When the original format was SRA, each datafile was pre-processed with standard tools in the
982 pipeline

```
983  
984 fastq-dump → bwa aln [genome.fa] → bwa samse → samtools view -bS -F 4  
985 → samtools sort → samtools index
```

986 to generate its associated BAM and BAI files. Otherwise, the tool

```
987  
988 bedtools multicov -bams [file.bam] -bed [bins_and_controlwindows.bed]
```

989 was applied (excluding failed-QC reads and duplicate reads by default) directly on the
990 original BAM²³ file to generate the corresponding read count file in BED format.
992

993 **RNA-seq data processing**

994 The processed data were mRNA abundances in FPKM at RefSeq TSSs. When the original format
995 was GTF (containing already FPKM values, as in the selected ENCODE RNA-seq datafiles
996 for *H. sapiens*), those values were used directly in the analysis. When the original format was
997 SAM, each datafile was pre-processed by first sorting it to generate then a BAM file using
998 `samtools view -bS`. If otherwise the original format was BAM, mRNA levels at RefSeq TSSs
999 were then calculated with FPKM as unit using *Cufflinks* [76] directly on the original file with the
1000 following options:

1001

²³The BAI file is required implicitly.

```
1002 -GTF-guide <reference_annotation.(gtf/gff)>
1003 -frag-bias-correct <genome.fa>
1004 -multi-read-correct■
1005
```

1006 When the same TSS (i.e. same genomic coordinate and strand) displayed more than one identified
1007 transcript in the *Cufflinks* output, the respective FPKM values were added. Also, when replicates
1008 were available the measure of central tendency used was the median of the replicate FPKM
1009 values.

1010 Preparation of data input tables

1011 For each of the three species, all TSS_{def}—defined as those TSSs with measured mRNA abundance
1012 (i.e. FPKM > 0) in all cell types/cell samples—were determined. The number of TSS_{def} found
1013 for each species were $N_{\text{TSS}_{\text{def}}}(\textit{Homo sapiens}) = 14,742$, $N_{\text{TSS}_{\text{def}}}(\textit{Mus musculus}) = 16,021$, and
1014 $N_{\text{TSS}_{\text{def}}}(\textit{Drosophila melanogaster}) = 11,632$. Then, for each cell type/cell sample, 30 genomic
1015 bins were defined and denoted by the distance (in bp) between their 5'-end and their respective
1016 TSS_{def} genomic coordinate: “-2000”, “-1800”, “-1600”, “-1400”, “-1200”, “-1000”, “-800”,
1017 “-600”, “-400”, “-200”, “0” (TSS_{def} or ‘+1’), “200”, “400”, “600”, “800”, “1000”, “1200”,
1018 “1400”, “1600”, “1800”, “2000”, “2200”, “2400”, “2600”, “2800”, “3000”, “3200”, “3400”,
1019 “3600”, and “3800”. Then, for each cell type/cell sample, a ChIP-seq read signal was computed
1020 for all bins in all TSS_{def} genomic regions (e.g. in the “-2000” bin of the *Homo sapiens* TSS with
1021 RefSeq ID: NM_001127328, H3K27ac₋₂₀₀₀ = 4.68 in H1-hESC stem cells). Data input tables,
1022 with n_m being the number of histone H3 modifications comprised, were generated following this
1023 structure of rows and columns²⁴:

	H3[1] ₋₂₀₀₀	...	H3[n_m] ₋₂₀₀₀	...	H3[1] ₃₈₀₀	...	H3[n_m] _{3,800}	FPKM
1								
1024	:							
	$N_{\text{TSS}_{\text{def}}}$							

1025 The tables were written then to these data files:

1026 ***H. sapiens***: Hs_Gm12878.dat, Hs_H1hesc.dat, Hs_Hsmm.dat, Hs_Huvec.dat,
1027 Hs_Nhek.dat, Hs_Nhlf.dat■

1028 ***M. musculus***: Mm_Heart.dat, Mm_Liver.dat, Mm_E14-d0.dat, Mm_E14-d4.dat,
1029 Mm_E14-d6.dat■

1030 ***D. melanogaster***: Dm_E0-4.dat, Dm_E4-8.dat, Dm_E8-12.dat, Dm_E12-16.dat,
1031 Dm_E16-20.dat, Dm_E20-24.dat, Dm_L1.dat, Dm_L2.dat,
1032 Dm_Pupae.dat■

²⁴For reference, additional columns were appended in the generated .dat files after the FPKM column with the chromosome, position, strand and RefSeq ID of each TSS_{def}.

1033 Computation of *ctalk_non_epi* profiles

1034 If the variables X_j (representing the signal for histone H3 modification X in the genomic bin
 1035 $j \in \{-2000, \dots, 3800\}$), Y_k (representing the signal for histone H3 modification Y in the
 1036 genomic bin $k \in \{-2000, \dots, 3800\}$) and Z (representing FPKM values) are random variables,
 1037 then the covariance of X_j and Y_k can be decomposed directly in terms of their linear relationship
 1038 with Z as the sum

$$\text{Cov}(X_j, Y_k) = \underbrace{\frac{\text{Cov}(X_j, Z)\text{Cov}(Y_k, Z)}{\text{Var}(Z)}}_{\substack{\text{covariance of } X_j \text{ and } Y_k \\ \text{resulting from their} \\ \text{linear relationship with } Z}} + \underbrace{\text{Cov}(X_j, Y_k|Z)}_{\substack{\text{covariance of } X_j \text{ and } Y_k \\ \text{orthogonal to } Z}}, \quad (1)$$

1039 where the second summand $\text{Cov}(X_j, Y_k|Z)$ is the partial covariance between X_j and Y_k given Z .
 1040 It is easy to see that $\text{Cov}(X_j, Y_k|Z)$ is a local approximation of Nanny’s constraints C_N on
 1041 histone H3 modifications, as anticipated in the preliminary theoretical definitions²⁵. To make the
 1042 *ctalk_non_epi* profiles comparable however, $\text{Cov}(X_j, Y_k|Z)$ values have to be normalized²⁶ by the
 1043 standard deviations of the residuals of X_j and Y_k with respect to Z . In other words, the partial
 1044 correlation $\text{Cor}(X_j, Y_k|Z)$ values were needed. Nevertheless, a correlation value does not have a
 1045 straightforward interpretation, whereas its square—typically known as *coefficient of determination*,
 1046 *effect size of the correlation*, or simply r^2 —does: it represents the relative (i.e. fraction of) variance
 1047 of one random variable explained by the other. For this reason, $\text{Cor}(X_j, Y_k|Z)^2$ was used to
 1048 represent the strength of the association, and then multiplied by the sign of the correlation to
 1049 represent the direction of the association. Thus, after \log_2 -transforming the X_j , Y_k and Z data,
 1050 each pairwise combination of bin-specific histone H3 modifications $\{X_j, Y_k\}$ contributed with the
 1051 value

$$\text{ctalk_non_epi}(X_j, Y_k) = \underbrace{\text{sgn}(\text{Cor}(X_j, Y_k|Z))}_{\substack{\text{partial correlation} \\ \text{sign} \in \{-1, 1\}}} \underbrace{(\text{Cor}(X_j, Y_k|Z))^2}_{\substack{\text{partial correlation} \\ \text{strength} \in [-1, 1]}}. \quad (2)$$

1052 This implies that for each pairwise combination of histone H3 modifications $\{X, Y\}$, there
 1053 are 30 (bins for X) \times 30 (bins for Y) = 900 (bin-combination-specific *ctalk_non_epi* values).
 1054 To increase the robustness of the analysis against the departures of the actual nucleosome
 1055 distributions from the 30×200 -bp bins model, the values were then sorted in descending order
 1056 and placed in a 900-tuple.

²⁵A straightforward corollary is that Waddington’s constraints C_W can in turn be approximated locally by $\frac{\text{Cov}(X_j, Z)\text{Cov}(Y_k, Z)}{\text{Var}(Z)}$.

²⁶At the cost of losing the sum decomposition property, which was used here for explanatory purposes.

1057 For a cell type/cell sample from a species with data for n_m histone H3 modifications,
1058 e.g. $n_m(\textit{Mus musculus}) = 5$, the length of the final *ctalk_non_epi* profile comprising all
1059 possible $\{X, Y\}$ combinations would be ${}^{n_m}C_2 \times 900$. However, a final data filtering was
1060 performed.

1061 The justification for this additional filtering was that some pairwise partial
1062 correlation values were expected a priori to be strong and significant, which was
1063 later confirmed. Namely, (i) those involving the same histone H3 modification in
1064 the same amino acid residue (e.g. $\text{Cor}(\text{H3K9ac}_{-200}, \text{H3K9ac}_{-400} | \text{FPKM}) > 0$;
1065 $\text{Cor}(\text{H3K4me3}_{-200}, \text{H3K4me3}_{-200} | \text{FPKM}) = 1$) (ii) those involving a
1066 different type of histone H3 modification in the same amino acid residue
1067 (e.g. $\text{Cor}(\text{H3K27ac}_{-800}, \text{H3K27me3}_{-600} | \text{FPKM}) < 0$), and (iii) those involving
1068 the same type of histone H3 modification in the same amino acid residue
1069 (e.g. $\text{Cor}(\text{H3K4me2}_{-400}, \text{H3K4me3}_{-400} | \text{FPKM}) > 0$) in part because ChIP-antibody
1070 cross reactivity has been shown able to introduce artifacts on the accurate assessment of
1071 some histone-crosstalk associations [20, 21]. For these reasons, in each species all pairwise
1072 combinations of histone H3 modifications involving the same amino acid residue were then
1073 identified as “trivial” and excluded from the *ctalk_non_epi* profiles construction. E.g., since
1074 for *Mus musculus* the comprised histone modifications were H3K4me1, H3K4me3, H3K27ac,
1075 H3K27me3, and H3K36me3 ($n_m = 5$), the pairwise combinations H3K4me1–H3K4me3 and
1076 H3K27ac–H3K27me3 were filtered out. Therefore, the length of the *Mus musculus ctalk_non_epi*
1077 profiles was $({}^5C_2 - 2) \times 900 = 7,200$.

1078 Statistical significance assessment

1079 The statistical significance of the partial correlation $\text{Cor}(X_j, Y_k | Z)$ values, necessary for
1080 constructing the *ctalk_non_epi* profiles, was estimated using Fisher’s z-transformation [77]. Under
1081 the null hypothesis $\text{Cor}(X_j, Y_k | Z) = 0$ the statistic $z = \sqrt{N_{\text{TSS}_{\text{def}}} - |Z| - 3} \frac{1}{2} \ln \left(\frac{1 + \text{Cor}(X_j, Y_k | Z)}{1 - \text{Cor}(X_j, Y_k | Z)} \right)$,
1082 where $N_{\text{TSS}_{\text{def}}}$ is the sample size and $|Z| = 1$ (i.e. one control variable), follows asymptotically a
1083 $N(0, 1)$ distribution. The p-values can be then computed easily using the $N(0, 1)$ probability
1084 function.

1085 Multiple comparisons correction of the p-values associated to each *ctalk_non_epi* profile was
1086 performed using the Benjamini-Yekutieli method [78]. The parameter used was the number of all
1087 possible²⁷ comparisons: $({}^{n_m \times 30}C_2)$. From the resulting q-values associated to each *ctalk_non_epi*
1088 profile an empirical cumulative distribution was obtained, which in turn was used to compute
1089 a threshold t . The value of t was optimized to be the maximum value such that within the
1090 q-values smaller than t is expected less than 1 false-positive partial correlation. Consequently,
1091 if $\text{q-value}[i] \geq t$ then the associated partial correlation value was identified as not significant
1092 (i.e. zero) in the respective *ctalk_non_epi* profile.

²⁷Before excluding “trivial” pairwise combinations of histone H3 modifications, to further increase the conservativeness of the correction.

1093 Unsupervised hierarchical clustering of *ctalk_non_epi* and mRNA 1094 abundance profiles

1095 The goal of this step was to evaluate the significant *ctalk_non_epi*-profile clusters—if any—in the
1096 phenograms (i.e. “phenotypic similarity dendrograms”) obtained from unsupervised hierarchical
1097 clustering analyses (unsupervised HCA). For each species, the analyses were conducted on
1098 (i) the *ctalk_non_epi* profiles of each cell type/sample (Figure 1A, 1C, and 1E) and (ii) the
1099 \log_2 -transformed FPKM profiles (i.e mRNA abundance) of each cell type/sample (Figure 1B, 1D,
1100 and 1F). Important to the HCA technique is the choice of a metric (for determining the distance
1101 between any two profiles) and a cluster-linkage method (for determining the distance between
1102 any two clusters).

1103 Different ChIP-seq antibodies display differential binding affinities (with respect to different
1104 epitopes or even the same epitope, depending on the manufacturer) that are intrinsic and
1105 irrespective to the biological phenomenon of interest. For this reason, comparing directly
1106 the strengths (i.e. magnitudes) in the *ctalk_non_epi* profiles (e.g. using Euclidean distance as
1107 metric) is to introduce significant biases in the analysis. In contrast, the “correlation distance”
1108 metric—customarily used for comparing gene expression profiles—defined between any two
1109 profiles $pro[i], pro[j]$ as

$$d_r(pro[i], pro[j]) = 1 - \text{Cor}(pro[i], pro[j]) \quad (3)$$

1110 compares instead the “shape” of the profiles²⁸, hence it was the metric used here. On the other
1111 hand, the cluster-linkage method chosen was the “average” method or UPGMA (Unweighted Pair
1112 Group Method with Arithmetic Mean) in which the distance $D(A, B)$ between any clusters A and
1113 B is defined as

$$D(A, B) = \frac{1}{|A||B|} \sum_{\substack{pro[k] \in A \\ pro[l] \in B}} d_r(pro[k], pro[l]), \quad (4)$$

1114 that is, the mean of all distances $d_r(pro[k], pro[l])$ such that $pro[k] \in A$ and $pro[l] \in B$ (this
1115 method was chosen because it has been shown to yield the highest cophenetic correlation values
1116 when using the “correlation distance” metric [79]). Cluster statistical significance was assessed as
1117 *au* (approximately unbiased) and *bp* (bootstrap probability) significance scores by non-parametric
1118 bootstrap resampling using the *Pvclust* [24] add-on package for the *R* software [80]. The number
1119 of bootstrap replicates in each analysis was 10,000.

²⁸ As a consequence of what was highlighted previously, the “correlation distance” metric is also invariant under linear transformations of the profiles.

1120 Suitability of FPKM as unit of mRNA abundance

1121 Previous research has pinpointed that FPKM may not always be an adequate unit of transcript
1122 abundance in differential expression studies. It was shown that, if transcript size distribution
1123 varies significantly among the samples, FPKM/RPKM²⁹ will introduce biases. For this reason
1124 another abundance unit TPM (transcripts per million)—which is a linear transformation of the
1125 FPKM value for each sample—was proposed to overcome the limitation [81]. However, this issue
1126 was not a problem for this study.

1127 This is because partial correlation, used to construct the *ctalk_non_epi* profiles later
1128 subject to HCA, is invariant under linear transformations of the control variable Z
1129 (i.e. $\text{Cor}(X_j, Y_k|Z) = \text{Cor}(X_j, Y_k|aZ + b)$ for any two scalars $\{a, b\}$). Importantly, this property
1130 also implies that *ctalk_non_epi* profiles are controlling not only for mRNA abundance but also
1131 for any other biological variable displaying a strong linear relationship with mRNA abundance
1132 (e.g. chromatin accessibility represented by DNase I hypersensitivity, as shown in [20]). Similarly,
1133 the unsupervised hierarchical clustering of mRNA abundance profiles is invariant under linear
1134 transformations of the profiles, since $\text{Cor}(Z_i, Z_j) = \text{Cor}(aZ_i + b, cZ_j + d)$ provided $ac > 0$.

²⁹Reads per transcript kilobase per million fragments mapped.

1135 **Acknowledgements**

1136 I wish to thank the following people:

- 1137 • John Tyler Dodge, horn soloist at the *Orquesta Filarmónica de Santiago*, for reviewing most
1138 of the English in this paper and his valuable questions, which pushed me to the limit of my
1139 abilities in the purpose of making this paper self-explanatory.
- 1140 • Miguel Allende, director of the FONDAP Center for Genome Regulation (see details in the
1141 institutional acknowledgements below).
- 1142 • Alejandro Maass, professor at the Center for Mathematical Modeling (CMM), Universidad
1143 de Chile, for his special interest in this work and his interesting questions.
- 1144 • My anonymous colleagues who reviewed the grant proposal on behalf of FONDECYT (see
1145 below).

1146

1147 Also, I wish to thank the following institutions:

- 1148 • The National Fund for Scientific and Technological Development (FONDECYT, Chile) for
1149 the postdoctoral grant (see details in [Funding](#)).
- 1150 • Universidad Andrés Bello and its Faculty of Biological Sciences for sponsoring my
1151 postdoctoral grant proposal to FONDECYT.
- 1152 • The FONDAP Center for Genome Regulation (CGR, Chile) for generously granting me a
1153 workplace for more than a year and giving me the opportunity to share some preliminary
1154 results of this work with other colleagues at the CGR.
- 1155 • The National Laboratory for High Performance Computing (NLHPC, Chile) for providing
1156 me with a free academic account, which helped me carry out efficiently most of the
1157 computational analyses described in this paper.
- 1158 • The *Math^{omics}* Lab (Chile), for kindly helping me with the setup of my NLHPC account.

1159 **Additional information**

1160 No institution (including the funder) or person other than the author had any role in
1161 study conception, design, publicly-available data collection, computational analysis, theory
1162 development, paper writing, or the decision to submit this preprint to bioRxiv.

1163 **Copyright**

1164 The copyright holder for this preprint is the author. It is made made available under the
1165 Creative Commons Attribution 4.0 International License. To view a copy of this license, visit
1166 <http://creativecommons.org/licenses/by/4.0/>.

1167



1168

1169 **Funding**

	Funder	Grant reference number	Author
1170	National Fund for Scientific and Technological Development (FONDECYT)	3140328	Felipe A. Veloso

1171 References

- 1172 [1] Slack JMW (2002) Timeline: Conrad Hal Waddington: the last renaissance biologist? *Nat*
1173 *Rev Genet* 3: 889–895. doi: [10.1038/nrg933](https://doi.org/10.1038/nrg933).
- 1174 [2] Waddington CH (1957) *The strategy of the genes: a discussion of some aspects of theoretical*
1175 *biology*. London: Allen & Unwin.
- 1176 [3] Takahashi K, Yamanaka S (2006) Induction of pluripotent stem cells from mouse embryonic
1177 and adult fibroblast cultures by defined factors. *Cell* 126: 663–676. doi:
1178 [10.1016/j.cell.2006.07.024](https://doi.org/10.1016/j.cell.2006.07.024).
- 1179 [4] Wolffe AP (1999) Epigenetics: Regulation through repression. *Science* 286: 481–486. doi:
1180 [10.1126/science.286.5439.481](https://doi.org/10.1126/science.286.5439.481).
- 1181 [5] Bonasio R, Tu S, Reinberg D (2010) Molecular signals of epigenetic states. *Science* 330:
1182 612–6. doi: [10.1126/science.1191078](https://doi.org/10.1126/science.1191078).
- 1183 [6] Kamakura M (2011) Royalactin induces queen differentiation in honeybees. *Nature* 473:
1184 478–483. doi: [10.1038/nature10093](https://doi.org/10.1038/nature10093).
- 1185 [7] Fraser P (2010). Defining epigenetics. Interviews by G. Riddihough. *Science* [Video podcast]
1186 00:05:34–00:05:47. URL <http://videolab.sciencemag.org/featured/650920373001/1>.
- 1187 [8] Orphanides G, Reinberg D (2002) A unified theory of gene expression. *Cell* 108: 439–451.
1188 doi: [10.1016/s0092-8674\(02\)00655-4](https://doi.org/10.1016/s0092-8674(02)00655-4).
- 1189 [9] Li G, Reinberg D (2011) Chromatin higher-order structures and gene regulation. *Current*
1190 *Opinion in Genetics & Development* 21: 175–186. doi: [10.1016/j.gde.2011.01.022](https://doi.org/10.1016/j.gde.2011.01.022).
- 1191 [10] Cope NF, Fraser P, Eskiw CH (2010) The yin and yang of chromatin spatial organization.
1192 *Genome Biol* 11: 204. doi: [10.1186/gb-2010-11-3-204](https://doi.org/10.1186/gb-2010-11-3-204).
- 1193 [11] Ralston A, Shaw K (2008) Gene expression regulates cell differentiation. *Nat Educ* 1: 127.
1194 URL [http:](http://www.nature.com/scitable/topicpage/gene-expression-regulates-cell-differentiation-931)
1195 [//www.nature.com/scitable/topicpage/gene-expression-regulates-cell-differentiation-931](http://www.nature.com/scitable/topicpage/gene-expression-regulates-cell-differentiation-931).
- 1196 [12] Berger SL, Kouzarides T, Shiekhhattar R, Shilatifard A (2009) An operational definition of
1197 epigenetics. *Genes & Development* 23: 781–783. doi: [10.1101/gad.1787609](https://doi.org/10.1101/gad.1787609).
- 1198 [13] Reinberg D (2010). Defining epigenetics. Interviews by G. Riddihough. *Science* [Video
1199 podcast] 00:01:25–00:01:35. URL <http://videolab.sciencemag.org/featured/650920373001/1>.
- 1200 [14] Arnone MI, Davidson EH (1997) The hardwiring of development: organization and function
1201 of genomic regulatory systems. *Development* 124: 1851–64.
- 1202 [15] Rose LS, Kempthues KJ (1998) Early patterning of the *C. elegans* embryo. *Annual Review of*
1203 *Genetics* 32: 521–545. doi: [10.1146/annurev.genet.32.1.521](https://doi.org/10.1146/annurev.genet.32.1.521).

- 1204 [16] Ladewig J, Koch P, Brüstle O (2013) Leveling waddington: the emergence of direct
1205 programming and the loss of cell fate hierarchies. *Nature Reviews Molecular Cell Biology* 14:
1206 225–236. doi: [10.1038/nrm3543](https://doi.org/10.1038/nrm3543).
- 1207 [17] Nanney DL (1958) Epigenetic control systems. *Proceedings of the National Academy of*
1208 *Sciences* 44: 712–717. doi: [10.1073/pnas.44.7.712](https://doi.org/10.1073/pnas.44.7.712).
- 1209 [18] Huang S (2012) The molecular and mathematical basis of waddington's epigenetic landscape:
1210 a framework for post-darwinian biology? *Bioessays* 34: 149-57. doi: [10.1002/bies.201100031](https://doi.org/10.1002/bies.201100031).
- 1211 [19] Kumar V, Muratani M, Rayan NA, Kraus P, Lufkin T, et al. (2013) Uniform, optimal signal
1212 processing of mapped deep-sequencing data. *Nat Biotechnol* 31: 615–622. doi:
1213 [10.1038/nbt.2596](https://doi.org/10.1038/nbt.2596).
- 1214 [20] Lasserre J, Chung HR, Vingron M (2013) Finding associations among histone modifications
1215 using sparse partial correlation networks. *PLoS Comput Biol* 9: e1003168. doi:
1216 [10.1371/journal.pcbi.1003168](https://doi.org/10.1371/journal.pcbi.1003168).
- 1217 [21] Peach SE, Rudomin EL, Udeshi ND, Carr SA, Jaffe JD (2012) Quantitative assessment of
1218 chromatin immunoprecipitation grade antibodies directed against histone modifications
1219 reveals patterns of co-occurring marks on histone protein molecules. *Mol Cell Proteomics* 11:
1220 128-37. doi: [10.1074/mcp.M111.015941](https://doi.org/10.1074/mcp.M111.015941).
- 1221 [22] Schwammle V, Aspalter CM, Sidoli S, Jensen ON (2014) Large scale analysis of co-existing
1222 post-translational modifications in histone tails reveals global fine structure of cross-talk.
1223 *Molecular & Cellular Proteomics* 13: 1855–1865. doi: [10.1074/mcp.o113.036335](https://doi.org/10.1074/mcp.o113.036335).
- 1224 [23] Zheng Y, Sweet SMM, Popovic R, Martinez-Garcia E, Tipton JD, et al. (2012) Total kinetic
1225 analysis reveals how combinatorial methylation patterns are established on lysines 27 and
1226 36 of histone h3. *Proc Natl Acad Sci U S A* 109: 13549-54. doi: [10.1073/pnas.1205707109](https://doi.org/10.1073/pnas.1205707109).
- 1227 [24] Suzuki R, Shimodaira H (2006) Pvclust: an r package for assessing the uncertainty in
1228 hierarchical clustering. *Bioinformatics* 22: 1540–1542. doi: [10.1093/bioinformatics/btl117](https://doi.org/10.1093/bioinformatics/btl117).
- 1229 [25] White KP (1999) Microarray analysis of *Drosophila* development during metamorphosis.
1230 *Science* 286: 2179–2184. doi: [10.1126/science.286.5447.2179](https://doi.org/10.1126/science.286.5447.2179).
- 1231 [26] Cantera R, Ferreiro MJ, Aransay AM, Barrio R (2014) Global gene expression shift during
1232 the transition from early neural development to late neuronal differentiation in drosophila
1233 melanogaster. *PLoS ONE* 9: e97703. doi: [10.1371/journal.pone.0097703](https://doi.org/10.1371/journal.pone.0097703).
- 1234 [27] Mody M, Cao Y, Cui Z, Tay KY, Shyong A, et al. (2001) Genome-wide gene expression
1235 profiles of the developing mouse hippocampus. *Proceedings of the National Academy of*
1236 *Sciences* 98: 8862–8867. doi: [10.1073/pnas.141244998](https://doi.org/10.1073/pnas.141244998).
- 1237 [28] Fraser P, Bickmore W (2007) Nuclear organization of the genome and the potential for gene
1238 regulation. *Nature* 447: 413–417. doi: [10.1038/nature05916](https://doi.org/10.1038/nature05916).
- 1239 [29] Haeckel E (1874) Die gastraea-theorie, die phylogenetische classification des thierreichs und
1240 die homologie der keimblätter. *Jenaische Zeitschrift für Naturwissenschaft* 8: 1-55.
- 1241 [30] Hadzi J (1963) *The evolution of the Metazoa*. Macmillan.

- 1242 [31] Metschnikoff E (1886) Embryologische Studien an Medusen: ein Beitrag zur Genealogie der
1243 primitiv-Organ. A. Hölder.
- 1244 [32] Kirk DL (2005) A twelve-step program for evolving multicellularity and a division of labor.
1245 *Bioessays* 27: 299–310. doi: [10.1002/bies.20197](https://doi.org/10.1002/bies.20197).
- 1246 [33] Nielsen C (2008) Six major steps in animal evolution: are we derived sponge larvae?
1247 *Evolution & Development* 10: 241–257. doi: [10.1111/j.1525-142x.2008.00231.x](https://doi.org/10.1111/j.1525-142x.2008.00231.x).
- 1248 [34] Mikhailov KV, Konstantinova AV, Nikitin MA, Troshin PV, Rusin LY, et al. (2009) The
1249 origin of metazoa: a transition from temporal to spatial cell differentiation. *Bioessays* 31:
1250 758–68. doi: [10.1002/bies.200800214](https://doi.org/10.1002/bies.200800214).
- 1251 [35] Levin TC, Greaney AJ, Wetzel L, King N (2014) The rosetteless gene controls development
1252 in the choanoflagellate *S. rosetta*. *eLife* 3. doi: [10.7554/elife.04070](https://doi.org/10.7554/elife.04070).
- 1253 [36] Kupiec JJ (1997) A darwinian theory for the origin of cellular differentiation. *Molecular and*
1254 *General Genetics MGG* 255: 201–208. doi: [10.1007/s004380050490](https://doi.org/10.1007/s004380050490).
- 1255 [37] Paldi A (2012) What makes the cell differentiate? *Prog Biophys Mol Biol* 110: 41–3. doi:
1256 [10.1016/j.pbiomolbio.2012.04.003](https://doi.org/10.1016/j.pbiomolbio.2012.04.003).
- 1257 [38] Kim J (1999) Making sense of emergence. *Philosophical Studies* 95: 3–36. doi:
1258 [10.1023/a:1004563122154](https://doi.org/10.1023/a:1004563122154).
- 1259 [39] Kim J (2006) Emergence: Core ideas and issues. *Synthese* 151: 547–559. doi:
1260 [10.1007/s11229-006-9025-0](https://doi.org/10.1007/s11229-006-9025-0).
- 1261 [40] Deacon TW (2012) *Incomplete nature: How mind emerged from matter*. New York: W.W.
1262 Norton & Co., 1st edition.
- 1263 [41] Chen L, Xiao S, Pang K, Zhou C, Yuan X (2014) Cell differentiation and germ-soma
1264 separation in ediacaran animal embryo-like fossils. *Nature* doi: [10.1038/nature13766](https://doi.org/10.1038/nature13766).
- 1265 [42] Meyerowitz EM (2002) Plants compared to animals: The broadest comparative study of
1266 development. *Science* 295: 1482–1485. doi: [10.1126/science.1066609](https://doi.org/10.1126/science.1066609).
- 1267 [43] Donoghue PCJ, Antcliffe JB (2010) Early life: Origins of multicellularity. *Nature* 466: 41–42.
1268 doi: [10.1038/466041a](https://doi.org/10.1038/466041a).
- 1269 [44] van Nimwegen E (2003) Scaling laws in the functional content of genomes. *Trends in*
1270 *Genetics* 19: 479–484. doi: [10.1016/s0168-9525\(03\)00203-8](https://doi.org/10.1016/s0168-9525(03)00203-8).
- 1271 [45] Young HE, Black AC (2003) Adult stem cells. *Anat Rec* 276A: 75–102. doi:
1272 [10.1002/ar.a.10134](https://doi.org/10.1002/ar.a.10134).
- 1273 [46] Cai S, Fu X, Sheng Z (2007) Dedifferentiation: A new approach in stem cell research.
1274 *BioScience* 57: 655. doi: [10.1641/b570805](https://doi.org/10.1641/b570805).
- 1275 [47] Donà E, Barry JD, Valentin G, Quirin C, Khmelinskii A, et al. (2013) Directional tissue
1276 migration through a self-generated chemokine gradient. *Nature* 503: 285–9. doi:
1277 [10.1038/nature12635](https://doi.org/10.1038/nature12635).

- 1278 [48] Venkiteswaran G, Lewellis SW, Wang J, Reynolds E, Nicholson C, et al. (2013) Generation
1279 and dynamics of an endogenous, self-generated signaling gradient across a migrating tissue.
1280 Cell 155: 674–687. doi: [10.1016/j.cell.2013.09.046](https://doi.org/10.1016/j.cell.2013.09.046).
- 1281 [49] Kauffman S, Clayton P (2006) On emergence, agency, and organization. Biology &
1282 Philosophy 21: 501–521. doi: [10.1007/s10539-005-9003-9](https://doi.org/10.1007/s10539-005-9003-9).
- 1283 [50] Combs PA, Eisen MB (2013) Sequencing mrna from cryo-sliced *Drosophila* embryos to
1284 determine genome-wide spatial patterns of gene expression. PLoS One 8: e71820. doi:
1285 [10.1371/journal.pone.0071820](https://doi.org/10.1371/journal.pone.0071820).
- 1286 [51] Wu AR, Neff NF, Kalisky T, Dalerba P, Treutlein B, et al. (2013) Quantitative assessment of
1287 single-cell RNA-sequencing methods. Nat Meth 11: 41–46. doi: [10.1038/nmeth.2694](https://doi.org/10.1038/nmeth.2694).
- 1288 [52] Roy S, Morse D (2012) A full suite of histone and histone modifying genes are transcribed in
1289 the dinoflagellate *Lingulodinium*. PLoS One 7: e34340. doi: [10.1371/journal.pone.0034340](https://doi.org/10.1371/journal.pone.0034340).
- 1290 [53] Meletis K, Barnabé-Heider F, Carlén M, Evergren E, Tomilin N, et al. (2008) Spinal cord
1291 injury reveals multilineage differentiation of ependymal cells. Plos Biol 6: e182. doi:
1292 [10.1371/journal.pbio.0060182](https://doi.org/10.1371/journal.pbio.0060182).
- 1293 [54] Sømme L (1982) Supercooling and winter survival in terrestrial arthropods. Comparative
1294 Biochemistry and Physiology Part A: Physiology 73: 519–543. doi:
1295 [10.1016/0300-9629\(82\)90260-2](https://doi.org/10.1016/0300-9629(82)90260-2).
- 1296 [55] Murphy WJ, Collier GE (1997) A molecular phylogeny for aplocheiloid fishes
1297 (atherinomorpha, cyprinodontiformes): the role of vicariance and the origins of annualism.
1298 Molecular Biology and Evolution 14: 790–799.
- 1299 [56] Niethammer P, Grabher C, Look AT, Mitchison TJ (2009) A tissue-scale gradient of
1300 hydrogen peroxide mediates rapid wound detection in zebrafish. Nature 459: 996–999. doi:
1301 [10.1038/nature08119](https://doi.org/10.1038/nature08119).
- 1302 [57] Unsworth BR, Lelkes PI (1998) Growing tissues in microgravity. Nat Med 4: 901–907. doi:
1303 [10.1038/nm0898-901](https://doi.org/10.1038/nm0898-901).
- 1304 [58] Correll MJ, Pyle TP, Millar KDL, Sun Y, Yao J, et al. (2013) Transcriptome analyses of
1305 arabidopsis thaliana seedlings grown in space: implications for gravity-responsive genes.
1306 Planta 238: 519–533. doi: [10.1007/s00425-013-1909-x](https://doi.org/10.1007/s00425-013-1909-x).
- 1307 [59] Hammond T, Lewis F, Goodwin T, Linnehan R, Wolf D, et al. (1999) Gene expression in
1308 space. Nature Medicine 5: 359–359. doi: [10.1038/7331](https://doi.org/10.1038/7331).
- 1309 [60] Crawford-Young SJ (2006) Effects of microgravity on cell cytoskeleton and embryogenesis.
1310 The International Journal of Developmental Biology 50: 183–191. doi: [10.1387/ijdb.052077sc](https://doi.org/10.1387/ijdb.052077sc).
- 1311 [61] Ingber D (1999) How cells (might) sense microgravity. The FASEB Journal 13: S3–S15.
- 1312 [62] Pojman JA, Bessonov N, Volpert V, Paley MS (2007) Miscible fluids in microgravity (MFMG):
1313 A zero-upmass investigation on the international space station. Microgravity Sci Technol 19:
1314 33–41. doi: [10.1007/bf02870987](https://doi.org/10.1007/bf02870987).

- 1315 [63] Rajjou L, Duval M, Gallardo K, Catusse J, Bally J, et al. (2012) Seed germination and vigor.
1316 *Annu Rev Plant Biol* 63: 507–533. doi: [10.1146/annurev-arplant-042811-105550](https://doi.org/10.1146/annurev-arplant-042811-105550).
- 1317 [64] Finch-Savage WE, Leubner-Metzger G (2006) Seed dormancy and the control of
1318 germination. *New Phytologist* 171: 501–523. doi: [10.1111/j.1469-8137.2006.01787.x](https://doi.org/10.1111/j.1469-8137.2006.01787.x).
- 1319 [65] Smet ID, Beeckman T (2011) Asymmetric cell division in land plants and algae: the driving
1320 force for differentiation. *Nature Reviews Molecular Cell Biology* 12: 177–188. doi:
1321 [10.1038/nrm3064](https://doi.org/10.1038/nrm3064).
- 1322 [66] Greenbaum D, Colangelo C, Williams K, Gerstein M (2003) Comparing protein abundance
1323 and mrna expression levels on a genomic scale. *Genome Biol* 4: 117.
- 1324 [67] Ning K, Fermin D, Nesvizhskii AI (2012) Comparative analysis of different label-free mass
1325 spectrometry based protein abundance estimates and their correlation with RNA-seq gene
1326 expression data. *J Proteome Res* 11: 2261–2271. doi: [10.1021/pr201052x](https://doi.org/10.1021/pr201052x).
- 1327 [68] Varela FG, Maturana HR, Uribe R (1974) Autopoiesis: the organization of living systems, its
1328 characterization and a model. *Biosystems* 5: 187–196.
- 1329 [69] Celniker SE, Dillon LAL, Gerstein MB, Gunsalus KC, Henikoff S, et al. (2009) Unlocking the
1330 secrets of the genome. *Nature* 459: 927–930. doi: [10.1038/459927a](https://doi.org/10.1038/459927a).
- 1331 [70] Ram O, Goren A, Amit I, Shores N, Yosef N, et al. (2011) Combinatorial patterning of
1332 chromatin regulators uncovered by genome-wide location analysis in human cells. *Cell* 147:
1333 1628–1639. doi: [10.1016/j.cell.2011.09.057](https://doi.org/10.1016/j.cell.2011.09.057).
- 1334 [71] Nègre N, Brown CD, Ma L, Bristow CA, Miller SW, et al. (2011) A cis-regulatory map of the
1335 *Drosophila* genome. *Nature* 471: 527–531. doi: [10.1038/nature09990](https://doi.org/10.1038/nature09990).
- 1336 [72] Dunham I, Kundaje A, Aldred SF, Collins PJ, Davis CA, et al. (2012) An integrated
1337 encyclopedia of DNA elements in the human genome. *Nature* 489: 57–74. doi:
1338 [10.1038/nature11247](https://doi.org/10.1038/nature11247).
- 1339 [73] Xiao S, Xie D, Cao X, Yu P, Xing X, et al. (2012) Comparative epigenomic annotation of
1340 regulatory DNA. *Cell* 149: 1381–1392. doi: [10.1016/j.cell.2012.04.029](https://doi.org/10.1016/j.cell.2012.04.029).
- 1341 [74] Djebali S, Davis CA, Merkel A, Dobin A, Lassmann T, et al. (2012) Landscape of
1342 transcription in human cells. *Nature* 489: 101–108. doi: [10.1038/nature11233](https://doi.org/10.1038/nature11233).
- 1343 [75] Stamatoyannopoulos JA, Snyder M, Hardison R, Ren B, Gingeras T, et al. (2012) An
1344 encyclopedia of mouse DNA elements (mouse ENCODE). *Genome Biol* 13: 418. doi:
1345 [10.1186/gb-2012-13-8-418](https://doi.org/10.1186/gb-2012-13-8-418).
- 1346 [76] Trapnell C, Williams BA, Pertea G, Mortazavi A, Kwan G, et al. (2010) Transcript assembly
1347 and quantification by RNA-seq reveals unannotated transcripts and isoform switching
1348 during cell differentiation. *Nat Biotechnol* 28: 511–515. doi: [10.1038/nbt.1621](https://doi.org/10.1038/nbt.1621).
- 1349 [77] Fisher RA (1915) Frequency distribution of the values of the correlation coefficient in samples
1350 from an indefinitely large population. *Biometrika* : 507–521.

- 1351 [78] Benjamini Y, Yekutieli D (2001) The control of the false discovery rate in multiple testing
1352 under dependency. *Annals of statistics* : 1165–1188.
- 1353 [79] Saraçlı S, Doğan N, Doğan I (2013) Comparison of hierarchical cluster analysis methods by
1354 cophenetic correlation. *Journal of Inequalities and Applications* 2013: 203. doi:
1355 [10.1186/1029-242x-2013-203](https://doi.org/10.1186/1029-242x-2013-203).
- 1356 [80] R Core Team (2014) R: A Language and Environment for Statistical Computing. R
1357 Foundation for Statistical Computing, Vienna, Austria. URL <http://www.R-project.org/>.
- 1358 [81] Wagner GP, Kin K, Lynch VJ (2012) Measurement of mRNA abundance using RNA-seq
1359 data: RPKM measure is inconsistent among samples. *Theory Biosci* 131: 281–285. doi:
1360 [10.1007/s12064-012-0162-3](https://doi.org/10.1007/s12064-012-0162-3).
- 1361 [82] Shannon CE, Weaver W (1949) *The mathematical theory of communication*. Urbana:
1362 University of Illinois Press.
- 1363 [83] Watanabe S (1960) Information theoretical analysis of multivariate correlation. *IBM Journal*
1364 *of research and development* 4: 66–82.
- 1365 [84] Voss TC, Hager GL (2014) Dynamic regulation of transcriptional states by chromatin and
1366 transcription factors. *Nat Rev Genet* 15: 69-81. doi: [10.1038/nrg3623](https://doi.org/10.1038/nrg3623).
- 1367 [85] Altun Z, Hall D (2002). *Wormatlas*.

1368 Appendix

1369 Formal theoretical definitions and notation

1370 The following definitions and notation regard molecular dynamics and spatial topology. To avoid
1371 ambiguity, the definitions regarding molecular dynamics will be derived from instantaneously
1372 defined random variables—measurable only partially and approximately but easily imaginable
1373 from a fundamental point of view—using Shannon’s information theory [82] measures³⁰.
1374 For further explanatory convenience, these random variables will be seen sometimes as sets.
1375 Definitions regarding spatial topology will be derived from instantaneously-specified spherical
1376 coordinates given the spherical/circular symmetry that developing embryos and cell populations
1377 display in general. Additionally, a brief glossary will be provided with the most relevant notation
1378 and concepts, described there in less rigorous terms yet logically sufficient for the theoretical
1379 formulation. If desired, the reader may then skip to this glossary and return to the formal
1380 definitions at any point later.

1381 Spatial topology

1382 Let $X_{(1;t)}, \dots, X_{(n;t)}$ be all cells in a given organism or cell population³¹ of the eukaryotic
1383 species X at a given instant t , spatially-specified in spherical coordinates. These spherical
1384 coordinates are r (radial distance), θ (azimuthal angle), and ϕ (polar angle). The origin of the
1385 coordinate system is the centroid of the cell population or embryo. Let $r_{(n;t)}(X_{(1;t)}, \dots, X_{(n;t)})$
1386 be the radius of the entire cell population or embryo.

1388 **Definition Overall space:** $S_O(X_{(1;t)}, \dots, X_{(n;t)})$

1389
1390 $S_O(X_{(1;t)}, \dots, X_{(n;t)}) = \{(r, \theta, \phi) \mid r \leq 0 \leq r_{(n;t)}(X_{(1;t)}, \dots, X_{(n;t)}), 0 \leq \theta < 2\pi, 0 \leq \phi \leq \pi\}$;
1391 that is, the set of all points (r, θ, ϕ) within the radius $r_{(n;t)}$.

1392 **Remark** This is the space occupied by the entire cell population or embryo. It can be expressed
1393 as the sum of the space occupied by all individual cells in the population/embryo plus the
1394 associated extracellular space.

1396 **Definition Cell-occupied space:** $S_C(X_{(1;t)}, \dots, X_{(n;t)})$

1397 $S_C(X_{(1;t)}, \dots, X_{(n;t)}) = \{(r, \theta, \phi) \mid (r, \theta, \phi) \in \bigcup_{i=1}^n S_O(X_{(i;t)})\}$; that is, the union of the sets of
1398 points (r, θ, ϕ) spatially-specifying all n individual cells at a given instant t .

³⁰In a strict sense, molecular dynamics should be represented by multivariate random variables and as a consequence generalized measures (such as Watanabe’s total correlation [83]) of statistical dependence would be needed. Univariate random variables were preferred here for simplicity in the notation.

³¹A single cell or zygote will be considered a cell population where $n = 1$. All cells will be treated geometrically as spheres unless specified later. A dividing cell will be regarded as a single cell until division is complete.

1399 **Remark** This is the space occupied by all n individual cells in the population/embryo at a given
1400 instant t .

1401

1402 **Definition** *Extracellular space:* $S_E(X_{(1;t)}, \dots, X_{(n;t)})$

1403

1404 $S_E(X_{(1;t)}, \dots, X_{(n;t)}) = S_O(X_{(1;t)}, \dots, X_{(n;t)}) \setminus S_C(X_{(1;t)}, \dots, X_{(n;t)})$; that is, the set
1405 difference of S_O and S_C , i.e. the set of points (r, θ, ϕ) such that $(r, \theta, \phi) \in S_T(X_{(1;t)}, \dots, X_{(n;t)})$
1406 and $(r, \theta, \phi) \notin S_T(X_{(1;t)}, \dots, X_{(n;t)})$.

1407 **Remark** Whereas this may seem an over-formalized definition of the widely-known concept
1408 of extracellular space, the theory postulated here shows its usefulness for describing some
1409 corollaries rigorously.

1410

1411 Molecular dynamics

1412 Let $X_{(i;t)}$ be the i^{th} cell³² of a given organism or cell population of the eukaryotic
1413 species X at a given instant t , let $G(X_{(i;t)})$ be its genomic sequence, let $T(X_{(i;t)})$ be the
1414 instantaneous transcription rate at the transcription start site, let $F(X_{(i;t)})$ be its entire
1415 molecular phenotype spatially-specified with respect to the transcription start site (note that
1416 $F(X_{(i;t)})$ describes implicitly specific molecular abundances), let $F^\circ(X_{(i;t)})$ be the molecular
1417 phenotype of the nucleus of $X_{(i;t)}$, and let $F^\star(X_{(i;t)})$ be the cell's molecular phenotype that
1418 is membrane-exchangeable with the extracellular space S_E by facilitated diffusion (note that
1419 $F^\circ(X_{(i;t)}), F^\star(X_{(i;t)}) \subset F(X_{(i;t)})$). Importantly, the set $G(X_{(i;t)}) \cup T(X_{(i;t)}) \cup F(X_{(i;t)})$ describes
1420 an instantaneously realized state (of interest for this work), and it is not to be confused with a
1421 state space—the set of all realizable states—in dynamical systems theory. For notation simplicity,
1422 the argument $X_{(i;t)}$ will be implicit henceforth unless necessary.

1423

1424 **Definition** *Waddington's constraints* $C_W(X_{(i;t)}) = I(F; T|G)$; that is, the conditional mutual
1425 information between F° (spatially-specified nuclear phenotype) and T (instantaneous
1426 transcription rate at the TSS) given the value of G (genomic sequence).

1427 **Remark** Waddington's constraints can be equivalently expressed in terms of Shannon's
1428 conditional entropies as $C_W(X_{(i;t)}) = H(F^\circ|G) - H(F^\circ|T, G)$.

1429 **Remark** $C_W(X_{(i;t)})$ can be interpreted as a measure of the statistical dependence (i.e. constraint)
1430 between F° (spatially-specified nuclear phenotype) and T (transcription rates) for a given value
1431 of G .

1432 **Remark** These constraints are determined by (i) the spatial coordinates in F° with respect to
1433 the TSS and (ii) the specific affinities of DNA with respect to the phenotypic elements specified
1434 in F° for any given value of G .

1435

³²A dividing cell will be regarded as a single cell until division is complete.

1436 **Definition** Waddington's embodiens $F_W(X_{(i;t)})$ is the largest subset of $F^\circ(X_{(i;t)})$ such that
1437 $I(F_W; T|G) > 0$.

1438 **Remark** In data analysis, the set $F_w(X_{(i;t)})$ is a subset of $F_W(X_{(i;t)})$ if sample $I(F_w; T|G)$ is
1439 significantly greater than zero.

1440 **Remark** As mentioned earlier, the quantitative assessment of the hereby defined as Waddington's
1441 constraints has made possible to predict transcript abundance states from histone modification
1442 ChIP-seq enrichment profiles near TSSs with high accuracy ($R \sim 0.9$) [19].

1443 **Example** The previous remark implies the following: if T is approximated by transcript
1444 abundance and F_w is approximated by ChIP-seq enrichment, then histone H3 modifications can
1445 be specified as Waddington's embodiens F_W .

1446 **Remark** If $X_{(j,t+\Delta t)}$ is a daughter cell of $X_{(i;t)}$ and if there are two sets $F_h(X_{(i;t)}) \subseteq F_W(X_{(i;t)})$
1447 and $F_h(X_{(j,t+\Delta t)}) \subseteq F_W(X_{(j,t+\Delta t)})$ such that $I(F_h(X_{(i;t)}); F_h(X_{(j,t+\Delta t)})) > 0$ (i.e. if Waddington's
1448 constraints are propagated in a heritable manner), then $(F_h(X_{(i;t)}) \cup F_h(X_{(j,t+\Delta t)}))$ specifies
1449 spatially a set of molecular substrates E that is customarily labeled as "epigenetic regulators".
1450 Whereas this is a trivial corollary in its strict sense, it highlights the substrate-centered
1451 character—as opposed to constraint-centered—of the traditional approach known as epigenetic
1452 landscape. Additionally, this corollary reinforces a point raised in the [introduction](#): the
1453 misleading—and if taken in a strict sense, logically inconsistent—character of the "regulator"
1454 label on any molecular substrates satisfying the conditions that define the set E .

1455

1456 **Definition** Waddington's extracellular propagators $F_W^\rightarrow(X_{(i;t)})$ is the largest subset of $F^\star - F_W$
1457 such that there is a minimal time interval Δt and a quantity $I_{W(\Delta t)}^\rightarrow > 0$ for which
1458 $I(F_W(X_{(i;t+\Delta t)}); F_W^\rightarrow(X_{(i;t)})) = I_{W(t)} + I_{W(\Delta t)}^\rightarrow \implies I(F_W(X_{(i;t)}); F_W^\rightarrow(X_{(i;t)})) = I_{W(t)}$; that is, the
1459 largest subset of F^\star that is not a subset of Waddington's embodiens F_W at the instant t but
1460 elicits a significant change (measurable as the mutual information $I_{W(\Delta t)}^\rightarrow$) in Waddington's
1461 embodiens F_W observable after Δt .

1462 **Remark** In data analysis, the set $F_w^\rightarrow(X_{(i;t)})$ is a subset of $F_W^\rightarrow(X_{(i;t)})$ if sample
1463 $I(F_W(X_{(i;t+\Delta t)}); F_w^\rightarrow(X_{(i;t)})) - I(F_W(X_{(i;t)}); F_w^\rightarrow(X_{(i;t)}))$ is significantly greater than zero and if
1464 the logical implication in the definition (i.e. causality) can be then inferred given the experimental
1465 design.

1466 **Remark** Note that if $F_W^\rightarrow(X_{(i;t)}) \neq \emptyset$, then the alleles specified in G must account for all
1467 gene products in F (spatially-specified phenotype) necessary for the facilitated diffusion of the
1468 molecules specified in $F_W^\rightarrow(X_{(i;t)})$ (e.g. functional and sufficiently abundant protein pores or
1469 carriers, or intracellular transducers if needed).

1470 **Remark** Waddington's extracellular propagators F_W^\rightarrow may need a certain set of Waddington's
1471 intracellular propagators (defined with respect to the set $F - (F^\star \cup F_W)$) to satisfy their own
1472 defining condition.

1473 **Definition** *Nanney's constraints* $C_N(X_{(i;t)}) = I(F^\circ; F_W|T)$; that is, the conditional mutual
1474 information between F° (spatially-specified nuclear phenotype) and F_W (Waddington's
1475 propagators) given the value of T (instantaneous transcription rate at the TSS).

1476 **Remark** Nanney's constraints can be equivalently expressed in terms of Shannon's conditional
1477 entropies as $C_N(X_{(i;t)}) = H(F^\circ|T) - H(F^\circ|F_W, T)$.

1478 **Remark** $C_N(X_{(i;t)})$ can be interpreted as a measure of the statistical dependence (i.e. constraint)
1479 between F° (spatially-specified nuclear phenotype) and F_W (Waddington's propagators) for a
1480 given value of T .

1481 **Remark** These constraints are determined by (i) the spatial coordinates in F° and Waddington's
1482 propagators F_W with respect to each other and (ii) the kinetic and structural constraints
1483 governing the interactions between Waddington's propagators in F_W and the entire nuclear
1484 phenotype in F° for any given value of T .

1485

1486 **Definition** *Nanney's embodiars* $F_N(X_{(i;t)})$ is the largest subset of F° such that $I(F_N; F_W|T) > 0$.

1487 **Remark** In data analysis, the set $F_n(X_{(i;t)})$ is a subset of $F_N(X_{(i;t)})$ if sample $I(F_n; F_W|T)$ is
1488 significantly greater than zero.

1489 **Example** The work cited previously [19], which demonstrated the high predictive power
1490 of histone modification profiles on transcript abundance, did so developing a trainable
1491 multivariate linear regression model. In the work presented in this paper, such linearity and
1492 demonstrated predictive power together made it possible to represent Nanney's constraints with
1493 the *ctalk_non_epi* profiles (see Materials and Methods). In turn, the high statistical significance of
1494 these *ctalk_non_epi* profiles (shown previously in the results) implies that histone H3 modifications
1495 can be specified as Nanney's embodiars F_N .

1496 **Remark** At this point it is possible formalize what was highlighted in the beginning of this
1497 discussion: if $X_{(i;t)}$ is a human, mouse, or fruit fly cell and F_{H3} is its set of histone H3
1498 modifications at transcription start sites, then $F_{H3} \subseteq (F_W(X_{(i;t)}) \cap F_N(X_{(i;t)}))$. In other words,
1499 histone H3 modifications at the TSS are specifiable as Waddington's embodiars F_W and as
1500 Nanney's embodiars F_N *simultaneously*. This critical result will be generalized theoretically for
1501 cells of any differentiated multicellular organism.

1502

1503 **Definition** *Nanney's extracellular propagators* $F_N^{\rightarrow}(X_{(i;t)})$ is the largest subset of $F^\star - F_N$
1504 such that there is a minimal time interval Δt and a quantity $I_{N(\Delta t)}^{\rightarrow} > 0$ for which
1505 $I(F_N(X_{(i;t+\Delta t)}); F_N^{\rightarrow}(X_{(i;t)})) = I_{N(t)} + I_{N(\Delta t)}^{\rightarrow} \implies I(F_N(X_{(i;t)}); F_N^{\rightarrow}(X_{(i;t)})) = I_{N(t)}$; that is, the
1506 largest subset of F^\star that is not a subset of Nanney's embodiars F_N at the instant t but elicits
1507 a significant change (measurable as the mutual information $I_{N(\Delta t)}^{\rightarrow}$) in Nanney's embodiars F_N
1508 observable after Δt .

1509 **Remark** In data analysis, the set F_n^{\rightarrow} is a subset of $F_n^{\rightarrow}(X_{(i;t)})$ if sample
1510 $I(F_N(X_{(i;t+\Delta t)}); F_n^{\rightarrow}(X_{(i;t)})) - I(F_N(X_{(i;t)}); F_n^{\rightarrow}(X_{(i;t)}))$ is significantly greater than zero and if
1511 the logical implication in the definition (i.e. causality) can be then inferred given the experimental
1512 design.

1513 **Remark** Note that if $F_N^{\rightarrow}(X_{(i;t)}) \neq \emptyset$, then the alleles specified in G must account for all
1514 gene products in F (spatially-specified phenotype) necessary for the facilitated diffusion of the
1515 molecules specified in $F_N^{\rightarrow}(X_{(i;t)})$ (e.g. functional and sufficiently abundant protein pores or
1516 carriers, or intracellular transducers if needed).

1517 **Remark** Nanney's extracellular propagators F_N^{\rightarrow} may need a certain set of Nanney's intracellular
1518 propagators (defined with respect to the set $F - (F^{\star} \cup F_N)$) to satisfy their own defining condition.

1519 **Remark** Whereas the existence of Nanney's extracellular propagators F_W^{\rightarrow} is indisputable [84], to
1520 my knowledge evidence for the existence of Nanney's extracellular propagators F_N^{\rightarrow} has not been
1521 searched for and thus, not surprisingly, is currently absent. However, the appearance of Nanney's
1522 extracellular propagators F_N^{\rightarrow} was a necessary condition for the evolution of differentiated
1523 multicellularity, as it is proposed in the theory.

1524 **Estimation of a lower bound for the necessary cell-fate information**
 1525 **capacity in the hermaphrodite *Caenorhabditis elegans* ontogeny**

Count		N ^o
Cells generated		1,090
Deaths in the process		131
Final cells		959
Cell types developed		19
(Data source: WormAtlas website [85])		
	Estimated as	N ^o (approx.)
Total divisions	$2^{\log_2(\text{cells_generated}+1)} - 1$	2,179
Cell-fate divisions	$2^{\log_2(\text{cell_types}+1)} - 1$	37
Non-cell-fate divisions	$\text{total_divisions} - (\text{cell_fate_divisions} + \text{deaths})$	2,011
	Estimated as	p $-p \log_2 p$
Cell death	$\text{deaths} / \text{total_divisions}$	0.060 0.244
1527 Non-cell-fate division	$\text{non_cell_fate_divisions} / \text{total_divisions}$	0.923 0.107
Cell-fate division	$\text{cell_fate_divisions} / \text{total_divisions}$	0.017 0.1
Uncertainty per division (Sum)		0.451
	Estimated as	(bit)
1528 Uncertainty to resolve (total)	$\text{uncertainty_per_division} \times \text{total_divisions}$	983

1529 Note: germ line cells were excluded from the analysis.

1530 **Supplementary Information**

1531 ***Homo sapiens* source data of ChIP-seq on histone H3 modifications**
 1532 **(BAM/BAI files) [70]**

1533 For downloading, the URL must be constructed by adding the following prefix to each file listed:

1534

1535 <ftp://hgdownload.cse.ucsc.edu/goldenPath/hg19/encodeDCC/wgEncodeBroadHistone/>

Cell type	Antibody	GEO Accession	File URL suffix
GM12878	H3K27ac	GSM733771	wgEncodeBroadHistoneGm12878H3k27acStdA1nRep1.bam.bai
GM12878	H3K27ac	GSM733771	wgEncodeBroadHistoneGm12878H3k27acStdA1nRep1.bam
GM12878	H3K27ac	GSM733771	wgEncodeBroadHistoneGm12878H3k27acStdA1nRep2.bam.bai
GM12878	H3K27ac	GSM733771	wgEncodeBroadHistoneGm12878H3k27acStdA1nRep2.bam
GM12878	H3K27me3	GSM733758	wgEncodeBroadHistoneGm12878H3k27me3StdA1nRep1.bam.bai
GM12878	H3K27me3	GSM733758	wgEncodeBroadHistoneGm12878H3k27me3StdA1nRep1.bam
GM12878	H3K27me3	GSM733758	wgEncodeBroadHistoneGm12878H3k27me3StdA1nRep2.bam.bai
GM12878	H3K27me3	GSM733758	wgEncodeBroadHistoneGm12878H3k27me3StdA1nRep2.bam
GM12878	H3K27me3	GSM733758	wgEncodeBroadHistoneGm12878H3k27me3StdA1nRep3V2.bam.bai
GM12878	H3K27me3	GSM733758	wgEncodeBroadHistoneGm12878H3k27me3StdA1nRep3V2.bam
GM12878	H3K36me3	GSM733679	wgEncodeBroadHistoneGm12878H3k36me3StdA1nRep1.bam.bai
GM12878	H3K36me3	GSM733679	wgEncodeBroadHistoneGm12878H3k36me3StdA1nRep1.bam
GM12878	H3K36me3	GSM733679	wgEncodeBroadHistoneGm12878H3k36me3StdA1nRep2.bam.bai
GM12878	H3K36me3	GSM733679	wgEncodeBroadHistoneGm12878H3k36me3StdA1nRep2.bam
GM12878	H3K4me1	GSM733772	wgEncodeBroadHistoneGm12878H3k4me1StdA1nRep2.bam.bai
GM12878	H3K4me1	GSM733772	wgEncodeBroadHistoneGm12878H3k4me1StdA1nRep2.bam
GM12878	H3K4me1	GSM733772	wgEncodeBroadHistoneGm12878H3k04me1StdA1nRep1V2.bam.bai
GM12878	H3K4me1	GSM733772	wgEncodeBroadHistoneGm12878H3k04me1StdA1nRep1V2.bam
GM12878	H3K4me2	GSM733769	wgEncodeBroadHistoneGm12878H3k4me2StdA1nRep1.bam.bai
GM12878	H3K4me2	GSM733769	wgEncodeBroadHistoneGm12878H3k4me2StdA1nRep1.bam
GM12878	H3K4me2	GSM733769	wgEncodeBroadHistoneGm12878H3k4me2StdA1nRep2.bam.bai
GM12878	H3K4me2	GSM733769	wgEncodeBroadHistoneGm12878H3k4me2StdA1nRep2.bam
GM12878	H3K4me3	GSM733708	wgEncodeBroadHistoneGm12878H3k04me3StdA1nRep2V2.bam.bai
GM12878	H3K4me3	GSM733708	wgEncodeBroadHistoneGm12878H3k04me3StdA1nRep2V2.bam
GM12878	H3K4me3	GSM733708	wgEncodeBroadHistoneGm12878H3k4me3StdA1nRep1.bam.bai
GM12878	H3K4me3	GSM733708	wgEncodeBroadHistoneGm12878H3k4me3StdA1nRep1.bam
GM12878	H3K79me2	GSM733736	wgEncodeBroadHistoneGm12878H3k79me2StdA1nRep1.bam.bai
GM12878	H3K79me2	GSM733736	wgEncodeBroadHistoneGm12878H3k79me2StdA1nRep1.bam
GM12878	H3K79me2	GSM733736	wgEncodeBroadHistoneGm12878H3k79me2StdA1nRep2.bam.bai
GM12878	H3K79me2	GSM733736	wgEncodeBroadHistoneGm12878H3k79me2StdA1nRep2.bam
GM12878	H3K9ac	GSM733677	wgEncodeBroadHistoneGm12878H3k9acStdA1nRep1.bam.bai
GM12878	H3K9ac	GSM733677	wgEncodeBroadHistoneGm12878H3k9acStdA1nRep1.bam
GM12878	H3K9ac	GSM733677	wgEncodeBroadHistoneGm12878H3k9acStdA1nRep2.bam.bai
GM12878	H3K9ac	GSM733677	wgEncodeBroadHistoneGm12878H3k9acStdA1nRep2.bam
GM12878	H3K9me3	GSM733664	wgEncodeBroadHistoneGm12878H3k9me3StdA1nRep1.bam.bai
GM12878	H3K9me3	GSM733664	wgEncodeBroadHistoneGm12878H3k9me3StdA1nRep1.bam
GM12878	H3K9me3	GSM733664	wgEncodeBroadHistoneGm12878H3k9me3StdA1nRep2.bam.bai
GM12878	H3K9me3	GSM733664	wgEncodeBroadHistoneGm12878H3k9me3StdA1nRep2.bam
GM12878	H3K9me3	GSM733664	wgEncodeBroadHistoneGm12878H3k9me3StdA1nRep3.bam.bai
GM12878	H3K9me3	GSM733664	wgEncodeBroadHistoneGm12878H3k9me3StdA1nRep3.bam

Continued on next page

Continued from previous page

Cell type	Antibody	GEO Accession	File URL suffix
GM12878	Input	GSM733742	wgEncodeBroadHistoneGm12878ControlStdA1nRep1.bam.bai
GM12878	Input	GSM733742	wgEncodeBroadHistoneGm12878ControlStdA1nRep1.bam
GM12878	Input	GSM733742	wgEncodeBroadHistoneGm12878ControlStdA1nRep2.bam.bai
GM12878	Input	GSM733742	wgEncodeBroadHistoneGm12878ControlStdA1nRep2.bam
H1-hESC	H3K27ac	GSM733718	wgEncodeBroadHistoneH1hescH3k27acStdA1nRep1.bam.bai
H1-hESC	H3K27ac	GSM733718	wgEncodeBroadHistoneH1hescH3k27acStdA1nRep1.bam
H1-hESC	H3K27ac	GSM733718	wgEncodeBroadHistoneH1hescH3k27acStdA1nRep2.bam.bai
H1-hESC	H3K27ac	GSM733718	wgEncodeBroadHistoneH1hescH3k27acStdA1nRep2.bam
H1-hESC	H3K27me3	GSM733748	wgEncodeBroadHistoneH1hescH3k27me3StdA1nRep1.bam.bai
H1-hESC	H3K27me3	GSM733748	wgEncodeBroadHistoneH1hescH3k27me3StdA1nRep1.bam
H1-hESC	H3K27me3	GSM733748	wgEncodeBroadHistoneH1hescH3k27me3StdA1nRep2.bam.bai
H1-hESC	H3K27me3	GSM733748	wgEncodeBroadHistoneH1hescH3k27me3StdA1nRep2.bam
H1-hESC	H3K36me3	GSM733725	wgEncodeBroadHistoneH1hescH3k36me3StdA1nRep1.bam.bai
H1-hESC	H3K36me3	GSM733725	wgEncodeBroadHistoneH1hescH3k36me3StdA1nRep1.bam
H1-hESC	H3K36me3	GSM733725	wgEncodeBroadHistoneH1hescH3k36me3StdA1nRep2.bam.bai
H1-hESC	H3K36me3	GSM733725	wgEncodeBroadHistoneH1hescH3k36me3StdA1nRep2.bam
H1-hESC	H3K4me1	GSM733782	wgEncodeBroadHistoneH1hescH3k4me1StdA1nRep1.bam.bai
H1-hESC	H3K4me1	GSM733782	wgEncodeBroadHistoneH1hescH3k4me1StdA1nRep1.bam
H1-hESC	H3K4me1	GSM733782	wgEncodeBroadHistoneH1hescH3k4me1StdA1nRep2.bam.bai
H1-hESC	H3K4me1	GSM733782	wgEncodeBroadHistoneH1hescH3k4me1StdA1nRep2.bam
H1-hESC	H3K4me2	GSM733670	wgEncodeBroadHistoneH1hescH3k4me2StdA1nRep1.bam.bai
H1-hESC	H3K4me2	GSM733670	wgEncodeBroadHistoneH1hescH3k4me2StdA1nRep1.bam
H1-hESC	H3K4me2	GSM733670	wgEncodeBroadHistoneH1hescH3k4me2StdA1nRep2.bam.bai
H1-hESC	H3K4me2	GSM733670	wgEncodeBroadHistoneH1hescH3k4me2StdA1nRep2.bam
H1-hESC	H3K4me3	GSM733657	wgEncodeBroadHistoneH1hescH3k4me3StdA1nRep1.bam.bai
H1-hESC	H3K4me3	GSM733657	wgEncodeBroadHistoneH1hescH3k4me3StdA1nRep1.bam
H1-hESC	H3K4me3	GSM733657	wgEncodeBroadHistoneH1hescH3k4me3StdA1nRep2.bam.bai
H1-hESC	H3K4me3	GSM733657	wgEncodeBroadHistoneH1hescH3k4me3StdA1nRep2.bam
H1-hESC	H3K79me2	GSM1003547	wgEncodeBroadHistoneH1hescH3k79me2StdA1nRep1.bam.bai
H1-hESC	H3K79me2	GSM1003547	wgEncodeBroadHistoneH1hescH3k79me2StdA1nRep1.bam
H1-hESC	H3K79me2	GSM1003547	wgEncodeBroadHistoneH1hescH3k79me2StdA1nRep2.bam.bai
H1-hESC	H3K79me2	GSM1003547	wgEncodeBroadHistoneH1hescH3k79me2StdA1nRep2.bam
H1-hESC	H3K9ac	GSM733773	wgEncodeBroadHistoneH1hescH3k9acStdA1nRep1.bam.bai
H1-hESC	H3K9ac	GSM733773	wgEncodeBroadHistoneH1hescH3k9acStdA1nRep1.bam
H1-hESC	H3K9ac	GSM733773	wgEncodeBroadHistoneH1hescH3k9acStdA1nRep2.bam.bai
H1-hESC	H3K9ac	GSM733773	wgEncodeBroadHistoneH1hescH3k9acStdA1nRep2.bam
H1-hESC	H3K9me3	GSM1003585	wgEncodeBroadHistoneH1hescH3k09me3StdA1nRep1.bam.bai
H1-hESC	H3K9me3	GSM1003585	wgEncodeBroadHistoneH1hescH3k09me3StdA1nRep1.bam
H1-hESC	H3K9me3	GSM1003585	wgEncodeBroadHistoneH1hescH3k09me3StdA1nRep2.bam.bai
H1-hESC	H3K9me3	GSM1003585	wgEncodeBroadHistoneH1hescH3k09me3StdA1nRep2.bam
H1-hESC	Input	GSM733770	wgEncodeBroadHistoneH1hescControlStdA1nRep1.bam.bai
H1-hESC	Input	GSM733770	wgEncodeBroadHistoneH1hescControlStdA1nRep1.bam
H1-hESC	Input	GSM733770	wgEncodeBroadHistoneH1hescControlStdA1nRep2.bam.bai
H1-hESC	Input	GSM733770	wgEncodeBroadHistoneH1hescControlStdA1nRep2.bam
HSM1	H3K27ac	GSM733755	wgEncodeBroadHistoneHsmmH3k27acStdA1nRep1.bam.bai
HSM1	H3K27ac	GSM733755	wgEncodeBroadHistoneHsmmH3k27acStdA1nRep1.bam
HSM1	H3K27ac	GSM733755	wgEncodeBroadHistoneHsmmH3k27acStdA1nRep2.bam.bai
HSM1	H3K27ac	GSM733755	wgEncodeBroadHistoneHsmmH3k27acStdA1nRep2.bam
HSM1	H3K27me3	GSM733667	wgEncodeBroadHistoneHsmmH3k27me3StdA1nRep1.bam.bai
HSM1	H3K27me3	GSM733667	wgEncodeBroadHistoneHsmmH3k27me3StdA1nRep1.bam
HSM1	H3K27me3	GSM733667	wgEncodeBroadHistoneHsmmH3k27me3StdA1nRep2.bam.bai

Continued on next page

Continued from previous page

Cell type	Antibody	GEO Accession	File URL suffix
HSMM	H3K27me3	GSM733667	wgEncodeBroadHistoneHsmmH3k27me3StdA1nRep2.bam
HSMM	H3K36me3	GSM733702	wgEncodeBroadHistoneHsmmH3k36me3StdA1nRep1.bam.bai
HSMM	H3K36me3	GSM733702	wgEncodeBroadHistoneHsmmH3k36me3StdA1nRep1.bam
HSMM	H3K36me3	GSM733702	wgEncodeBroadHistoneHsmmH3k36me3StdA1nRep2.bam.bai
HSMM	H3K36me3	GSM733702	wgEncodeBroadHistoneHsmmH3k36me3StdA1nRep2.bam
HSMM	H3K4me1	GSM733761	wgEncodeBroadHistoneHsmmH3k4me1StdA1nRep1.bam.bai
HSMM	H3K4me1	GSM733761	wgEncodeBroadHistoneHsmmH3k4me1StdA1nRep1.bam
HSMM	H3K4me1	GSM733761	wgEncodeBroadHistoneHsmmH3k4me1StdA1nRep2.bam.bai
HSMM	H3K4me1	GSM733761	wgEncodeBroadHistoneHsmmH3k4me1StdA1nRep2.bam
HSMM	H3K4me2	GSM733768	wgEncodeBroadHistoneHsmmH3k4me2StdA1nRep1.bam.bai
HSMM	H3K4me2	GSM733768	wgEncodeBroadHistoneHsmmH3k4me2StdA1nRep1.bam
HSMM	H3K4me2	GSM733768	wgEncodeBroadHistoneHsmmH3k4me2StdA1nRep2.bam.bai
HSMM	H3K4me2	GSM733768	wgEncodeBroadHistoneHsmmH3k4me2StdA1nRep2.bam
HSMM	H3K4me3	GSM733637	wgEncodeBroadHistoneHsmmH3k4me3StdA1nRep1.bam.bai
HSMM	H3K4me3	GSM733637	wgEncodeBroadHistoneHsmmH3k4me3StdA1nRep1.bam
HSMM	H3K4me3	GSM733637	wgEncodeBroadHistoneHsmmH3k4me3StdA1nRep2.bam.bai
HSMM	H3K4me3	GSM733637	wgEncodeBroadHistoneHsmmH3k4me3StdA1nRep2.bam
HSMM	H3K79me2	GSM733741	wgEncodeBroadHistoneHsmmH3k79me2StdA1nRep1.bam.bai
HSMM	H3K79me2	GSM733741	wgEncodeBroadHistoneHsmmH3k79me2StdA1nRep1.bam
HSMM	H3K79me2	GSM733741	wgEncodeBroadHistoneHsmmH3k79me2StdA1nRep2.bam.bai
HSMM	H3K79me2	GSM733741	wgEncodeBroadHistoneHsmmH3k79me2StdA1nRep2.bam
HSMM	H3K9ac	GSM733775	wgEncodeBroadHistoneHsmmH3k9acStdA1nRep1.bam.bai
HSMM	H3K9ac	GSM733775	wgEncodeBroadHistoneHsmmH3k9acStdA1nRep1.bam
HSMM	H3K9ac	GSM733775	wgEncodeBroadHistoneHsmmH3k9acStdA1nRep2.bam.bai
HSMM	H3K9ac	GSM733775	wgEncodeBroadHistoneHsmmH3k9acStdA1nRep2.bam
HSMM	H3K9me3	GSM733730	wgEncodeBroadHistoneHsmmH3k9me3StdA1nRep1.bam.bai
HSMM	H3K9me3	GSM733730	wgEncodeBroadHistoneHsmmH3k9me3StdA1nRep1.bam
HSMM	H3K9me3	GSM733730	wgEncodeBroadHistoneHsmmH3k9me3StdA1nRep2.bam.bai
HSMM	H3K9me3	GSM733730	wgEncodeBroadHistoneHsmmH3k9me3StdA1nRep2.bam
HSMM	Input	GSM733663	wgEncodeBroadHistoneHsmmControlStdA1nRep1.bam.bai
HSMM	Input	GSM733663	wgEncodeBroadHistoneHsmmControlStdA1nRep1.bam
HSMM	Input	GSM733663	wgEncodeBroadHistoneHsmmControlStdA1nRep2.bam.bai
HSMM	Input	GSM733663	wgEncodeBroadHistoneHsmmControlStdA1nRep2.bam
HUVEC	H3K27ac	GSM733691	wgEncodeBroadHistoneHuvecH3k27acStdA1nRep1.bam.bai
HUVEC	H3K27ac	GSM733691	wgEncodeBroadHistoneHuvecH3k27acStdA1nRep1.bam
HUVEC	H3K27ac	GSM733691	wgEncodeBroadHistoneHuvecH3k27acStdA1nRep2.bam.bai
HUVEC	H3K27ac	GSM733691	wgEncodeBroadHistoneHuvecH3k27acStdA1nRep2.bam
HUVEC	H3K27ac	GSM733691	wgEncodeBroadHistoneHuvecH3k27acStdA1nRep3.bam.bai
HUVEC	H3K27ac	GSM733691	wgEncodeBroadHistoneHuvecH3k27acStdA1nRep3.bam
HUVEC	H3K27me3	GSM733688	wgEncodeBroadHistoneHuvecH3k27me3StdA1nRep1.bam.bai
HUVEC	H3K27me3	GSM733688	wgEncodeBroadHistoneHuvecH3k27me3StdA1nRep1.bam
HUVEC	H3K27me3	GSM733688	wgEncodeBroadHistoneHuvecH3k27me3StdA1nRep2.bam.bai
HUVEC	H3K27me3	GSM733688	wgEncodeBroadHistoneHuvecH3k27me3StdA1nRep2.bam
HUVEC	H3K36me3	GSM733757	wgEncodeBroadHistoneHuvecH3k36me3StdA1nRep1.bam.bai
HUVEC	H3K36me3	GSM733757	wgEncodeBroadHistoneHuvecH3k36me3StdA1nRep1.bam
HUVEC	H3K36me3	GSM733757	wgEncodeBroadHistoneHuvecH3k36me3StdA1nRep2.bam.bai
HUVEC	H3K36me3	GSM733757	wgEncodeBroadHistoneHuvecH3k36me3StdA1nRep2.bam
HUVEC	H3K36me3	GSM733757	wgEncodeBroadHistoneHuvecH3k36me3StdA1nRep3.bam.bai
HUVEC	H3K36me3	GSM733757	wgEncodeBroadHistoneHuvecH3k36me3StdA1nRep3.bam
HUVEC	H3K4me1	GSM733690	wgEncodeBroadHistoneHuvecH3k4me1StdA1nRep1.bam.bai
HUVEC	H3K4me1	GSM733690	wgEncodeBroadHistoneHuvecH3k4me1StdA1nRep1.bam

Continued on next page

Continued from previous page

Cell type	Antibody	GEO Accession	File URL suffix
HUVEC	H3K4me1	GSM733690	wgEncodeBroadHistoneHuvecH3k4me1StdA1nRep2.bam.bai
HUVEC	H3K4me1	GSM733690	wgEncodeBroadHistoneHuvecH3k4me1StdA1nRep2.bam
HUVEC	H3K4me1	GSM733690	wgEncodeBroadHistoneHuvecH3k4me1StdA1nRep3.bam.bai
HUVEC	H3K4me1	GSM733690	wgEncodeBroadHistoneHuvecH3k4me1StdA1nRep3.bam
HUVEC	H3K4me2	GSM733683	wgEncodeBroadHistoneHuvecH3k4me2StdA1nRep1.bam.bai
HUVEC	H3K4me2	GSM733683	wgEncodeBroadHistoneHuvecH3k4me2StdA1nRep1.bam
HUVEC	H3K4me2	GSM733683	wgEncodeBroadHistoneHuvecH3k4me2StdA1nRep2.bam.bai
HUVEC	H3K4me2	GSM733683	wgEncodeBroadHistoneHuvecH3k4me2StdA1nRep2.bam
HUVEC	H3K4me3	GSM733673	wgEncodeBroadHistoneHuvecH3k4me3StdA1nRep1.bam.bai
HUVEC	H3K4me3	GSM733673	wgEncodeBroadHistoneHuvecH3k4me3StdA1nRep1.bam
HUVEC	H3K4me3	GSM733673	wgEncodeBroadHistoneHuvecH3k4me3StdA1nRep2.bam.bai
HUVEC	H3K4me3	GSM733673	wgEncodeBroadHistoneHuvecH3k4me3StdA1nRep2.bam
HUVEC	H3K4me3	GSM733673	wgEncodeBroadHistoneHuvecH3k4me3StdA1nRep3.bam.bai
HUVEC	H3K4me3	GSM733673	wgEncodeBroadHistoneHuvecH3k4me3StdA1nRep3.bam
HUVEC	H3K79me2	GSM1003555	wgEncodeBroadHistoneHuvecH3k79me2A1nRep1.bam.bai
HUVEC	H3K79me2	GSM1003555	wgEncodeBroadHistoneHuvecH3k79me2A1nRep1.bam
HUVEC	H3K79me2	GSM1003555	wgEncodeBroadHistoneHuvecH3k79me2A1nRep2.bam.bai
HUVEC	H3K79me2	GSM1003555	wgEncodeBroadHistoneHuvecH3k79me2A1nRep2.bam
HUVEC	H3K9ac	GSM733735	wgEncodeBroadHistoneHuvecH3k9acStdA1nRep1.bam.bai
HUVEC	H3K9ac	GSM733735	wgEncodeBroadHistoneHuvecH3k9acStdA1nRep1.bam
HUVEC	H3K9ac	GSM733735	wgEncodeBroadHistoneHuvecH3k9acStdA1nRep2.bam.bai
HUVEC	H3K9ac	GSM733735	wgEncodeBroadHistoneHuvecH3k9acStdA1nRep2.bam
HUVEC	H3K9ac	GSM733735	wgEncodeBroadHistoneHuvecH3k9acStdA1nRep3.bam.bai
HUVEC	H3K9ac	GSM733735	wgEncodeBroadHistoneHuvecH3k9acStdA1nRep3.bam
HUVEC	H3K9me3	GSM1003517	wgEncodeBroadHistoneHuvecH3k09me3A1nRep1.bam.bai
HUVEC	H3K9me3	GSM1003517	wgEncodeBroadHistoneHuvecH3k09me3A1nRep1.bam
HUVEC	H3K9me3	GSM1003517	wgEncodeBroadHistoneHuvecH3k09me3A1nRep2.bam.bai
HUVEC	H3K9me3	GSM1003517	wgEncodeBroadHistoneHuvecH3k09me3A1nRep2.bam
HUVEC	Input	GSM733715	wgEncodeBroadHistoneHuvecControlStdA1nRep1.bam.bai
HUVEC	Input	GSM733715	wgEncodeBroadHistoneHuvecControlStdA1nRep1.bam
HUVEC	Input	GSM733715	wgEncodeBroadHistoneHuvecControlStdA1nRep2.bam.bai
HUVEC	Input	GSM733715	wgEncodeBroadHistoneHuvecControlStdA1nRep2.bam
HUVEC	Input	GSM733715	wgEncodeBroadHistoneHuvecControlStdA1nRep3.bam.bai
HUVEC	Input	GSM733715	wgEncodeBroadHistoneHuvecControlStdA1nRep3.bam
NHEK	H3K27ac	GSM733674	wgEncodeBroadHistoneNhekH3k27acStdA1nRep1.bam.bai
NHEK	H3K27ac	GSM733674	wgEncodeBroadHistoneNhekH3k27acStdA1nRep1.bam
NHEK	H3K27ac	GSM733674	wgEncodeBroadHistoneNhekH3k27acStdA1nRep2.bam.bai
NHEK	H3K27ac	GSM733674	wgEncodeBroadHistoneNhekH3k27acStdA1nRep2.bam
NHEK	H3K27ac	GSM733674	wgEncodeBroadHistoneNhekH3k27acStdA1nRep3.bam.bai
NHEK	H3K27ac	GSM733674	wgEncodeBroadHistoneNhekH3k27acStdA1nRep3.bam
NHEK	H3K27me3	GSM733701	wgEncodeBroadHistoneNhekH3k27me3StdA1nRep1.bam.bai
NHEK	H3K27me3	GSM733701	wgEncodeBroadHistoneNhekH3k27me3StdA1nRep1.bam
NHEK	H3K27me3	GSM733701	wgEncodeBroadHistoneNhekH3k27me3StdA1nRep2.bam.bai
NHEK	H3K27me3	GSM733701	wgEncodeBroadHistoneNhekH3k27me3StdA1nRep2.bam
NHEK	H3K27me3	GSM733701	wgEncodeBroadHistoneNhekH3k27me3StdA1nRep3.bam.bai
NHEK	H3K27me3	GSM733701	wgEncodeBroadHistoneNhekH3k27me3StdA1nRep3.bam
NHEK	H3K36me3	GSM733726	wgEncodeBroadHistoneNhekH3k36me3StdA1nRep1.bam.bai
NHEK	H3K36me3	GSM733726	wgEncodeBroadHistoneNhekH3k36me3StdA1nRep1.bam
NHEK	H3K36me3	GSM733726	wgEncodeBroadHistoneNhekH3k36me3StdA1nRep2.bam.bai
NHEK	H3K36me3	GSM733726	wgEncodeBroadHistoneNhekH3k36me3StdA1nRep2.bam
NHEK	H3K36me3	GSM733726	wgEncodeBroadHistoneNhekH3k36me3StdA1nRep3.bam.bai
NHEK	H3K36me3	GSM733726	wgEncodeBroadHistoneNhekH3k36me3StdA1nRep3.bam

Continued on next page

Continued from previous page

Cell type	Antibody	GEO Accession	File URL suffix
NHEK	H3K36me3	GSM733726	wgEncodeBroadHistoneNhekH3k36me3StdA1nRep3.bam
NHEK	H3K4me1	GSM733698	wgEncodeBroadHistoneNhekH3k4me1StdA1nRep1.bam.bai
NHEK	H3K4me1	GSM733698	wgEncodeBroadHistoneNhekH3k4me1StdA1nRep1.bam
NHEK	H3K4me1	GSM733698	wgEncodeBroadHistoneNhekH3k4me1StdA1nRep2.bam.bai
NHEK	H3K4me1	GSM733698	wgEncodeBroadHistoneNhekH3k4me1StdA1nRep2.bam
NHEK	H3K4me1	GSM733698	wgEncodeBroadHistoneNhekH3k4me1StdA1nRep3.bam.bai
NHEK	H3K4me1	GSM733698	wgEncodeBroadHistoneNhekH3k4me1StdA1nRep3.bam
NHEK	H3K4me2	GSM733686	wgEncodeBroadHistoneNhekH3k4me2StdA1nRep1.bam.bai
NHEK	H3K4me2	GSM733686	wgEncodeBroadHistoneNhekH3k4me2StdA1nRep1.bam
NHEK	H3K4me2	GSM733686	wgEncodeBroadHistoneNhekH3k4me2StdA1nRep2.bam.bai
NHEK	H3K4me2	GSM733686	wgEncodeBroadHistoneNhekH3k4me2StdA1nRep2.bam
NHEK	H3K4me2	GSM733686	wgEncodeBroadHistoneNhekH3k4me2StdA1nRep3.bam.bai
NHEK	H3K4me2	GSM733686	wgEncodeBroadHistoneNhekH3k4me2StdA1nRep3.bam
NHEK	H3K4me3	GSM733720	wgEncodeBroadHistoneNhekH3k4me3StdA1nRep1.bam.bai
NHEK	H3K4me3	GSM733720	wgEncodeBroadHistoneNhekH3k4me3StdA1nRep1.bam
NHEK	H3K4me3	GSM733720	wgEncodeBroadHistoneNhekH3k4me3StdA1nRep2.bam.bai
NHEK	H3K4me3	GSM733720	wgEncodeBroadHistoneNhekH3k4me3StdA1nRep2.bam
NHEK	H3K4me3	GSM733720	wgEncodeBroadHistoneNhekH3k4me3StdA1nRep3.bam.bai
NHEK	H3K4me3	GSM733720	wgEncodeBroadHistoneNhekH3k4me3StdA1nRep3.bam
NHEK	H3K79me2	GSM1003527	wgEncodeBroadHistoneNhekH3k79me2A1nRep1.bam.bai
NHEK	H3K79me2	GSM1003527	wgEncodeBroadHistoneNhekH3k79me2A1nRep1.bam
NHEK	H3K79me2	GSM1003527	wgEncodeBroadHistoneNhekH3k79me2A1nRep2.bam.bai
NHEK	H3K79me2	GSM1003527	wgEncodeBroadHistoneNhekH3k79me2A1nRep2.bam
NHEK	H3K9ac	GSM733665	wgEncodeBroadHistoneNhekH3k9acStdA1nRep1.bam.bai
NHEK	H3K9ac	GSM733665	wgEncodeBroadHistoneNhekH3k9acStdA1nRep1.bam
NHEK	H3K9ac	GSM733665	wgEncodeBroadHistoneNhekH3k9acStdA1nRep2.bam.bai
NHEK	H3K9ac	GSM733665	wgEncodeBroadHistoneNhekH3k9acStdA1nRep2.bam
NHEK	H3K9ac	GSM733665	wgEncodeBroadHistoneNhekH3k9acStdA1nRep3.bam.bai
NHEK	H3K9ac	GSM733665	wgEncodeBroadHistoneNhekH3k9acStdA1nRep3.bam
NHEK	H3K9me3	GSM1003528	wgEncodeBroadHistoneNhekH3k09me3A1nRep1.bam.bai
NHEK	H3K9me3	GSM1003528	wgEncodeBroadHistoneNhekH3k09me3A1nRep1.bam
NHEK	H3K9me3	GSM1003528	wgEncodeBroadHistoneNhekH3k09me3A1nRep2.bam.bai
NHEK	H3K9me3	GSM1003528	wgEncodeBroadHistoneNhekH3k09me3A1nRep2.bam
NHEK	Input	GSM733740	wgEncodeBroadHistoneNhekControlStdA1nRep1.bam.bai
NHEK	Input	GSM733740	wgEncodeBroadHistoneNhekControlStdA1nRep1.bam
NHEK	Input	GSM733740	wgEncodeBroadHistoneNhekControlStdA1nRep2.bam.bai
NHEK	Input	GSM733740	wgEncodeBroadHistoneNhekControlStdA1nRep2.bam
NHLF	H3K27ac	GSM733646	wgEncodeBroadHistoneNh1fH3k27acStdA1nRep1.bam.bai
NHLF	H3K27ac	GSM733646	wgEncodeBroadHistoneNh1fH3k27acStdA1nRep1.bam
NHLF	H3K27ac	GSM733646	wgEncodeBroadHistoneNh1fH3k27acStdA1nRep2.bam.bai
NHLF	H3K27ac	GSM733646	wgEncodeBroadHistoneNh1fH3k27acStdA1nRep2.bam
NHLF	H3K27me3	GSM733764	wgEncodeBroadHistoneNh1fH3k27me3StdA1nRep1.bam.bai
NHLF	H3K27me3	GSM733764	wgEncodeBroadHistoneNh1fH3k27me3StdA1nRep1.bam
NHLF	H3K27me3	GSM733764	wgEncodeBroadHistoneNh1fH3k27me3StdA1nRep2.bam.bai
NHLF	H3K27me3	GSM733764	wgEncodeBroadHistoneNh1fH3k27me3StdA1nRep2.bam
NHLF	H3K36me3	GSM733699	wgEncodeBroadHistoneNh1fH3k36me3StdA1nRep1.bam.bai
NHLF	H3K36me3	GSM733699	wgEncodeBroadHistoneNh1fH3k36me3StdA1nRep1.bam
NHLF	H3K36me3	GSM733699	wgEncodeBroadHistoneNh1fH3k36me3StdA1nRep2.bam.bai
NHLF	H3K36me3	GSM733699	wgEncodeBroadHistoneNh1fH3k36me3StdA1nRep2.bam
NHLF	H3K4me1	GSM733649	wgEncodeBroadHistoneNh1fH3k4me1StdA1nRep1.bam.bai
NHLF	H3K4me1	GSM733649	wgEncodeBroadHistoneNh1fH3k4me1StdA1nRep1.bam

Continued on next page

Continued from previous page

Cell type	Antibody	GEO Accession	File URL suffix
NHLF	H3K4me1	GSM733649	wgEncodeBroadHistoneNhlFh3k4me1StdA1nRep2.bam.bai
NHLF	H3K4me1	GSM733649	wgEncodeBroadHistoneNhlFh3k4me1StdA1nRep2.bam
NHLF	H3K4me2	GSM733781	wgEncodeBroadHistoneNhlFh3k4me2StdA1nRep1.bam.bai
NHLF	H3K4me2	GSM733781	wgEncodeBroadHistoneNhlFh3k4me2StdA1nRep1.bam
NHLF	H3K4me2	GSM733781	wgEncodeBroadHistoneNhlFh3k4me2StdA1nRep2.bam.bai
NHLF	H3K4me2	GSM733781	wgEncodeBroadHistoneNhlFh3k4me2StdA1nRep2.bam
NHLF	H3K4me3	GSM733723	wgEncodeBroadHistoneNhlFh3k4me3StdA1nRep1.bam.bai
NHLF	H3K4me3	GSM733723	wgEncodeBroadHistoneNhlFh3k4me3StdA1nRep1.bam
NHLF	H3K4me3	GSM733723	wgEncodeBroadHistoneNhlFh3k4me3StdA1nRep2.bam.bai
NHLF	H3K4me3	GSM733723	wgEncodeBroadHistoneNhlFh3k4me3StdA1nRep2.bam
NHLF	H3K79me2	GSM1003549	wgEncodeBroadHistoneNhlFh3k79me2A1nRep1.bam.bai
NHLF	H3K79me2	GSM1003549	wgEncodeBroadHistoneNhlFh3k79me2A1nRep1.bam
NHLF	H3K79me2	GSM1003549	wgEncodeBroadHistoneNhlFh3k79me2A1nRep2.bam.bai
NHLF	H3K79me2	GSM1003549	wgEncodeBroadHistoneNhlFh3k79me2A1nRep2.bam
NHLF	H3K9ac	GSM733652	wgEncodeBroadHistoneNhlFh3k9acStdA1nRep1.bam.bai
NHLF	H3K9ac	GSM733652	wgEncodeBroadHistoneNhlFh3k9acStdA1nRep1.bam
NHLF	H3K9ac	GSM733652	wgEncodeBroadHistoneNhlFh3k9acStdA1nRep2.bam.bai
NHLF	H3K9ac	GSM733652	wgEncodeBroadHistoneNhlFh3k9acStdA1nRep2.bam
NHLF	H3K9me3	GSM1003531	wgEncodeBroadHistoneNhlFh3k09me3A1nRep1.bam.bai
NHLF	H3K9me3	GSM1003531	wgEncodeBroadHistoneNhlFh3k09me3A1nRep1.bam
NHLF	H3K9me3	GSM1003531	wgEncodeBroadHistoneNhlFh3k09me3A1nRep2.bam.bai
NHLF	H3K9me3	GSM1003531	wgEncodeBroadHistoneNhlFh3k09me3A1nRep2.bam
NHLF	Input	GSM733731	wgEncodeBroadHistoneNhlFcontrolStdA1nRep1.bam.bai
NHLF	Input	GSM733731	wgEncodeBroadHistoneNhlFcontrolStdA1nRep1.bam
NHLF	Input	GSM733731	wgEncodeBroadHistoneNhlFcontrolStdA1nRep2.bam.bai
NHLF	Input	GSM733731	wgEncodeBroadHistoneNhlFcontrolStdA1nRep2.bam

1536

1537 ***Homo sapiens* source data of RNA-seq transcript abundance in FPKM**
 1538 **(GTF files) [74]**

1539 For downloading, the URL must be constructed by adding the following prefix to each file listed:

1540

1541 <ftp://hgdownload.cse.ucsc.edu/goldenPath/hg19/encodeDCC/wgEncodeCaltechRnaSeq/>

Cell type	GEO Accession	File URL suffix
GM12878	GSM958728	wgEncodeCaltechRnaSeqGm12878R2x75I1200TSSRep1V3.gtf.gz
GM12878	GSM958728	wgEncodeCaltechRnaSeqGm12878R2x75I1200TSSRep2V3.gtf.gz
H1-hESC	GSM958733	wgEncodeCaltechRnaSeqH1hescR2x75I1200TSSRep1V3.gtf.gz
H1-hESC	GSM958733	wgEncodeCaltechRnaSeqH1hescR2x75I1200TSSRep2V3.gtf.gz
H1-hESC	GSM958733	wgEncodeCaltechRnaSeqH1hescR2x75I1200TSSRep3V3.gtf.gz
H1-hESC	GSM958733	wgEncodeCaltechRnaSeqH1hescR2x75I1200TSSRep4V3.gtf.gz
HSMM	GSM958744	wgEncodeCaltechRnaSeqHsmmR2x75I1200TSSRep1V3.gtf.gz
HSMM	GSM958744	wgEncodeCaltechRnaSeqHsmmR2x75I1200TSSRep2V3.gtf.gz
HUVEC	GSM958734	wgEncodeCaltechRnaSeqHuvecR2x75I1200TSSRep1V3.gtf.gz
HUVEC	GSM958734	wgEncodeCaltechRnaSeqHuvecR2x75I1200TSSRep2V3.gtf.gz
NHEK	GSM958736	wgEncodeCaltechRnaSeqNhekR2x75I1200TSSRep1V3.gtf.gz

Continued on next page

Continued from previous page

Cell type	GEO Accession	File URL suffix
NHEK	GSM958736	wgEncodeCa1techRnaSeqNhekR2x75I1200TSSRep2V3.gtf.gz
NHLF	GSM958746	wgEncodeCa1techRnaSeqNh1fR2x75I1200TSSRep1V3.gtf.gz
NHLF	GSM958746	wgEncodeCa1techRnaSeqNh1fR2x75I1200TSSRep2V3.gtf.gz

1542

1543 ***Mus musculus* source data of ChIP-seq on histone H3 modifications (SRA**
 1544 **files) [75, 73]**

1545 For downloading, the URL must be constructed by adding the following prefix to each file listed:

1546

1547 `ftp://ftp-trace.ncbi.nlm.nih.gov/sra/sra-instant/reads/ByRun/sra/SRR/`

Cell type	Antibody	Rep #	GEO Accession	File URL suffix
E14	IgG	1	GSM881345	SRR414/SRR414932/SRR414932.sra
E14-day0	H3K27ac	1	GSM881349	SRR414/SRR414936/SRR414936.sra
E14-day0	H3K27me3	1	GSM881350	SRR414/SRR414937/SRR414937.sra
E14-day0	H3K36me3	1	GSM881351	SRR414/SRR414938/SRR414938.sra
E14-day0	H3K4me1	1	GSM881352	SRR414/SRR414939/SRR414939.sra
E14-day0	H3K4me3	1	GSM881354	SRR414/SRR414941/SRR414941.sra
E14-day4	H3K27ac	1	GSM881357	SRR414/SRR414945/SRR414945.sra
E14-day4	H3K27me3	1	GSM881358	SRR414/SRR414946/SRR414946.sra
E14-day4	H3K36me3	1	GSM881359	SRR414/SRR414947/SRR414947.sra
E14-day4	H3K4me1	1	GSM881360	SRR414/SRR414948/SRR414948.sra
E14-day4	H3K4me3	1	GSM881362	SRR414/SRR414950/SRR414950.sra
E14-day6	H3K27ac	1	GSM881366	SRR414/SRR414955/SRR414955.sra
E14-day6	H3K27me3	1	GSM881367	SRR414/SRR414956/SRR414956.sra
E14-day6	H3K36me3	1	GSM881368	SRR414/SRR414957/SRR414957.sra
E14-day6	H3K4me1	1	GSM881369	SRR414/SRR414958/SRR414958.sra
E14-day6	H3K4me3	1	GSM881371	SRR414/SRR414960/SRR414960.sra
Heart (8 wks/o)	H3K27ac	1	GSM1000093	SRR566/SRR566827/SRR566827.sra
Heart (8 wks/o)	H3K27ac	2	GSM1000093	SRR566/SRR566828/SRR566828.sra
Heart (8 wks/o)	H3K27me3	1	GSM1000131	SRR566/SRR566903/SRR566903.sra
Heart (8 wks/o)	H3K27me3	2	GSM1000131	SRR566/SRR566904/SRR566904.sra
Heart (8 wks/o)	H3K36me3	1	GSM1000130	SRR566/SRR566901/SRR566901.sra
Heart (8 wks/o)	H3K36me3	2	GSM1000130	SRR566/SRR566902/SRR566902.sra
Heart (8 wks/o)	H3K4me1	1	GSM769025	SRR317/SRR317255/SRR317255.sra
Heart (8 wks/o)	H3K4me1	2	GSM769025	SRR317/SRR317256/SRR317256.sra
Heart (8 wks/o)	H3K4me3	1	GSM769017	SRR317/SRR317239/SRR317239.sra
Heart (8 wks/o)	H3K4me3	2	GSM769017	SRR317/SRR317240/SRR317240.sra
Heart (8 wks/o)	Input	1	GSM769032	SRR317/SRR317269/SRR317269.sra
Heart (8 wks/o)	Input	2	GSM769032	SRR317/SRR317270/SRR317270.sra
Liver (8 wks/o)	H3K27ac	1	GSM1000140	SRR566/SRR566921/SRR566921.sra
Liver (8 wks/o)	H3K27ac	2	GSM1000140	SRR566/SRR566922/SRR566922.sra
Liver (8 wks/o)	H3K27me3	1	GSM1000150	SRR566/SRR566941/SRR566941.sra
Liver (8 wks/o)	H3K27me3	2	GSM1000150	SRR566/SRR566942/SRR566942.sra
Liver (8 wks/o)	H3K36me3	1	GSM1000151	SRR566/SRR566943/SRR566943.sra
Liver (8 wks/o)	H3K36me3	2	GSM1000151	SRR566/SRR566944/SRR566944.sra

Continued on next page

Continued from previous page

Cell type	Antibody	Rep #	GEO Accession	File URL suffix
Liver (8 wks/o)	H3K4me1	1	GSM769015	SRR317/SRR317235/SRR317235.sra
Liver (8 wks/o)	H3K4me1	2	GSM769015	SRR317/SRR317236/SRR317236.sra
Liver (8 wks/o)	H3K4me3	1	GSM769014	SRR317/SRR317233/SRR317233.sra
Liver (8 wks/o)	H3K4me3	2	GSM769014	SRR317/SRR317234/SRR317234.sra
Liver (8 wks/o)	Input	1	GSM769034	SRR317/SRR317273/SRR317273.sra
Liver (8 wks/o)	Input	2	GSM769034	SRR317/SRR317274/SRR317274.sra

1548

1549 ***Mus musculus* source data of RNA-seq (BAM files) [75, 73]**

1550 For downloading, the URL must be constructed by adding one of the two following prefixes to
1551 each file listed:

- 1552 1. <ftp://ftp.ncbi.nlm.nih.gov/geo/samples/GSM881nnn/>
1553 2. <ftp://hgdownload.cse.ucsc.edu/goldenPath/mm9/encodeDCC/wgEncodeLicrRnaSeq/>

Cell type	Rep #	GEO Accession	File URL suffix
E14-day0	1	GSM881355	[<i>prefix_1</i>]GSM881355/supp1/GSM881355_E14_RNA.bam.gz
E14-day4	1	GSM881364	[<i>prefix_1</i>]GSM881364/supp1/GSM881364_E14_RNA_d4.bam.gz
E14-day6	1	GSM881373	[<i>prefix_1</i>]GSM881373/supp1/GSM881373_E14_RNA_d6.bam.gz
Heart (8 wks/o)	1	GSM929707	[<i>prefix_2</i>]wgEncodeLicrRnaSeqHeartCellPapMAdult8wksC57b16A1nRep1.bam
Heart (8 wks/o)	2	GSM929707	[<i>prefix_2</i>]wgEncodeLicrRnaSeqHeartCellPapMAdult8wksC57b16A1nRep2.bam
Liver (8 wks/o)	1	GSM929711	[<i>prefix_2</i>]wgEncodeLicrRnaSeqLiverCellPapMAdult8wksC57b16A1nRep1.bam
Liver (8 wks/o)	2	GSM929711	[<i>prefix_2</i>]wgEncodeLicrRnaSeqLiverCellPapMAdult8wksC57b16A1nRep2.bam

1554

1555 ***Drosophila melanogaster* source data of ChIP-seq on histone H3
1556 modifications (SRA files) [69, 71]**

1557 For downloading, the URL must be constructed by adding the following prefix to each file listed:

- 1558 <ftp://ftp-trace.ncbi.nlm.nih.gov/sra/sra-instant/reads/ByRun/sra/SRR/SRR030/>
1559

Developmental time point/period	Antibody	GEO Accession	File URL suffix
0-4h embryos	H3K27ac	GSM401407	SRR030295/SRR030295.sra
0-4h embryos	H3K27me3	GSM439448	SRR030360/SRR030360.sra
0-4h embryos	H3K4me1	GSM401409	SRR030297/SRR030297.sra
0-4h embryos	H3K4me3	GSM400656	SRR030269/SRR030269.sra
0-4h embryos	H3K9ac	GSM401408	SRR030296/SRR030296.sra
0-4h embryos	H3K9me3	GSM439457	SRR030369/SRR030369.sra
0-4h embryos	Input	GSM400657	SRR030270/SRR030270.sra
4-8h embryos	H3K27ac	GSM401404	SRR030292/SRR030292.sra

Continued on next page

Continued from previous page

Developmental time point/period	Antibody	GEO Accession	File URL suffix
4-8h embryos	H3K27me3	GSM439447	SRR030359/SRR030359.sra
4-8h embryos	H3K4me1	GSM401406	SRR030294/SRR030294.sra
4-8h embryos	H3K4me3	GSM400674	SRR030287/SRR030287.sra
4-8h embryos	H3K9ac	GSM401405	SRR030293/SRR030293.sra
4-8h embryos	H3K9me3	GSM439456	SRR030368/SRR030368.sra
4-8h embryos	Input	GSM400675	SRR030288/SRR030288.sra
8-12h embryos	H3K27ac	GSM432583	SRR030332/SRR030332.sra
8-12h embryos	H3K27me3	GSM439446	SRR030358/SRR030358.sra
8-12h embryos	H3K4me1	GSM432593	SRR030342/SRR030342.sra
8-12h embryos	H3K4me3	GSM432585	SRR030334/SRR030334.sra
8-12h embryos	H3K9ac	GSM432592	SRR030341/SRR030341.sra
8-12h embryos	H3K9me3	GSM439455	SRR030367/SRR030367.sra
8-12h embryos	Input	GSM432636	SRR030346/SRR030346.sra
12-16h embryos	H3K27ac	GSM432582	SRR030331/SRR030331.sra
12-16h embryos	H3K27me3	GSM439445	SRR030357/SRR030357.sra
12-16h embryos	H3K4me1	GSM432591	SRR030340/SRR030340.sra
12-16h embryos	H3K4me3	GSM432580	SRR030329/SRR030329.sra
12-16h embryos	H3K9ac	GSM439458	SRR030370/SRR030370.sra
12-16h embryos	H3K9me3	GSM439454	SRR030366/SRR030366.sra
12-16h embryos	Input	GSM432634	SRR030344/SRR030344.sra
16-20h embryos	H3K27ac	GSM401401	SRR030289/SRR030289.sra
16-20h embryos	H3K27me3	GSM439444	SRR030356/SRR030356.sra
16-20h embryos	H3K4me1	GSM401403	SRR030291/SRR030291.sra
16-20h embryos	H3K4me3	GSM400658	SRR030271/SRR030271.sra
16-20h embryos	H3K9ac	GSM401402	SRR030290/SRR030290.sra
16-20h embryos	H3K9me3	GSM439453	SRR030365/SRR030365.sra
16-20h embryos	Input	GSM400659	SRR030272/SRR030272.sra
20-24h embryos	H3K27ac	GSM401423	SRR030311/SRR030311.sra
20-24h embryos	H3K27me3	GSM439443	SRR030355/SRR030355.sra
20-24h embryos	H3K4me1	GSM439464	SRR030376/SRR030376.sra
20-24h embryos	H3K4me3	GSM400672	SRR030285/SRR030285.sra
20-24h embryos	H3K9ac	GSM401424	SRR030312/SRR030312.sra
20-24h embryos	H3K9me3	GSM439452	SRR030364/SRR030364.sra
20-24h embryos	Input	GSM400673	SRR030286/SRR030286.sra
L1 larvae	H3K27ac	GSM432581	SRR030330/SRR030330.sra
L1 larvae	H3K27me3	GSM439442	SRR030354/SRR030354.sra
L1 larvae	H3K4me1	GSM432588	SRR030337/SRR030337.sra
L1 larvae	H3K4me3	GSM400662	SRR030275/SRR030275.sra
L1 larvae	H3K9ac	GSM401422	SRR030310/SRR030310.sra
L1 larvae	H3K9me3	GSM439451	SRR030363/SRR030363.sra
L1 larvae	Input	GSM400663	SRR030276/SRR030276.sra
L2 larvae	H3K27ac	GSM401419	SRR030307/SRR030307.sra
L2 larvae	H3K27me3	GSM439441	SRR030353/SRR030353.sra
L2 larvae	H3K4me1	GSM401421	SRR030309/SRR030309.sra
L2 larvae	H3K4me3	GSM400668	SRR030281/SRR030281.sra
L2 larvae	H3K9ac	GSM401420	SRR030308/SRR030308.sra
L2 larvae	H3K9me3	GSM439450	SRR030362/SRR030362.sra
L2 larvae	Input	GSM400669	SRR030282/SRR030282.sra
Pupae	H3K27ac	GSM401413	SRR030301/SRR030301.sra
Pupae	H3K27me3	GSM439439	SRR030351/SRR030351.sra
Pupae	H3K4me1	GSM401415	SRR030303/SRR030303.sra

Continued on next page

Continued from previous page

Developmental time point/period	Antibody	GEO Accession	File URL suffix
Pupae	H3K4me3	GSM400664	SRR030277/SRR030277.sra
Pupae	H3K9ac	GSM401414	SRR030302/SRR030302.sra
Pupae	H3K9me3	GSM439449	SRR030361/SRR030361.sra
Pupae	Input	GSM400665	SRR030278/SRR030278.sra

1560

1561 ***Drosophila melanogaster* source data of RNA-seq (SAM files) [69, 71]**

1562 For downloading, the URL must be constructed by adding the following prefix to each file listed:

1563

1564 `ftp://data.modencode.org/all_files/dmel-signal-1/`

Developmental time point/period	GEO Accession	File URL suffix
0-4h embryos	GSM451806	2010_0-4_accepted_hits.sam.gz
4-8h embryos	GSM451809	2019_4-8_accepted_hits.sam.gz
8-12h embryos	GSM451808	2020_8-12_accepted_hits.sam.gz
12-16h embryos	GSM451803	2021_12-16_accepted_hits.sam.gz
16-20h embryos	GSM451807	2022_16-20_accepted_hits.sam.gz
20-24h embryos	GSM451810	2023_20-24_accepted_hits.sam.gz
L1 larvae	GSM451811	2024_L1_accepted_hits.sam.gz
L2 larvae	GSM453867	2025_L2_accepted_hits.sam.gz
Pupae	GSM451813	2030_Pupae_accepted_hits.sam.gz

1565